Extended Data Table 2 | Phosphorylation of AMPK in AdipoR knock-down C2C12 myotubes

Compounds	pAMPK/AMPK (ratio)	
	unrelated siRNA	AdipoR1 siRNA
Control	1.00	0.96
No.101962	5.35	5.10
No.103694	4.67	3.34
No.108049	4.75	2.68
No.112254	3.70	2.07
No.165073	1.29	1.23
No.168198	4.53	2.97
No.171723	2.13	2.39
No.171819	1.56	1.81
No.181432	2.03	2.40
No.182368	2.69	3.00
No.183665	2.88	2.83
No.189474	2.00	1.62
No.189640	1.85	1.82
No.191294	3.25	3.54
No.194936	2.11	2.49
No.195218	1.75	2.00
No.195831	2.88	2.98
No.196462	2.06	2.58
No.197248	2.09	2.55
No.197372	1.78	1.96
No.198637	2.24	2.51
No.200737	2.13	2.68
No.206685	1.76	2.39
No.209705	1.52	1.81
No.211156	2.36	2.59
No.214617	2.21	2.78
No.251327	2.85	3.15
No.260544	3.79	4.12
No.264785	3.70	3.58
No.268508	2.58	2.87
No.268949	3.10	2.82
No.272299	2.83	2.60
No.272350	2.03	2.54
No.274971	2.38	2.51
No.466151	2.22	1.94
No.473771	1.67	2.39
No.484140	2.34	2.30
No.492284	2.05	1.88
No.550212	1.91	2.14
Adiponectin	5.48	1.94

Phosphorylation of AMPK normalized to the amount of AMPK in C2C12 myotubes and transfected with or without the indicated siRNA duplex, treated for 5 min with adiponectin or the indicated small molecule.

Diabetologia (2012) 55:3350–3358
DOI 10.1007/s00125-012-2710-2

ARTICLE

Monocyte chemoattractant protein-1 (MCP-1) deficiency enhances alternatively activated M2 macrophages and ameliorates insulin resistance and fatty liver in lipoatrophic diabetic A-ZIP transgenic mice

Y. Nio · T. Yamauchi · M. Iwabu · M. Okada-Iwabu · M. Funata · M. Yamaguchi · K. Ueki · T. Kadowaki

Received: 7 May 2012 / Accepted: 24 July 2012 / Published online: 16 September 2012

Abstract
Aims/hypothesis Monocyte chemoattractant protein-1 (MCP-1)/chemokine (C-C motif) ligand (CCL) 2 (CCL2) secreted from white adipose tissue (WAT) in obesity has been reported to contribute to tissue macrophage accumulation and insulin resistance by inducing a chronic inflammatory state. MCP-1 has been shown to be elevated in the fatty liver of lipoatrophic A-ZIP-transgenic (A-ZIP-Tg) mice. Treatment of these mice with the CC chemokine receptor (CCR) 2 antagonist has been shown to ameliorate the hyperglycaemia, hyperinsulinaemia and hepatomegaly, in conjunction with reducing liver inflammation. However, since CCR2 antagonists can block not only MCP-1 but also MCP-2 (CCL8) and MCP-3 (CCL7), it remains unclear whether MCP-1 secreted from the liver could contribute to hyperglycaemia, hyperinsulinaemia and hepatomegaly in conjunction with liver inflammation, as well as to the M1 and M2 states of macrophage polarisation.
Methods To address these issues, we analysed the effects of targeted disruption of MCP-1 in A-ZIP-Tg mice.
Results MCP-1 deficiency alone or per se resulted in a significant amelioration of insulin resistance in A-ZIP-Tg mice, which was associated with a suppression of extracellular signal-regulated protein kinase (ERK)-1/2 and p38 mitogen-activated protein kinase (p38MAPK) phosphorylation in liver. Although MCP-1 deficiency did not reduce the expression of macrophage markers, it increased the expression of the genes encoding M2 macrophage markers such as *Arg1* and *Chi3l3*, as well as significantly reducing the triacylglycerol content of livers from A-ZIP-Tg mice.
Conclusions/ interpretation Our data clearly indicated that MCP-1 deficiency improved insulin resistance and hepatic steatosis in A-ZIP-Tg mice and was associated with switching macrophage polarisation and suppressing ERK-1/2 and p38MAPK phosphorylation.

Keywords A-ZIP-Tg mice · Extracellular signal-regulated protein kinase · Hepatic steatosis · Insulin signalling · Lipoatrophic diabetes · Macrophage polarisation · Monocyte chemoattractant protein-1

Abbreviations

p38MAPK	p38 Mitogen-activated protein kinase
ATMs	Adipose tissue macrophages
Arg1	Arginase-1
A-ZIP-Tg	A-ZIP-transgenic
A-ZIP-Tg×MCP1$^{-/-}$	A-ZIP transgenic MCP-1 homozygous knockout
BAT	Brown adipose tissue
Chi3l3	Chitinase 3-like 3

Electronic supplementary material The online version of this article (doi:10.1007/s00125-012-2710-2) contains peer-reviewed but unedited supplementary material, which is available to authorised users.

Y. Nio · T. Yamauchi (✉) · M. Iwabu · M. Okada-Iwabu · M. Funata · M. Yamaguchi · K. Ueki · T. Kadowaki (✉)
Department of Diabetes and Metabolic Diseases, Graduate School of Medicine, University of Tokyo, 7-3-1 Hongo, Bunkyo-ku, Tokyo 113-0033, Japan
e-mail: tyamau-tky@umin.net
e-mail: kadowaki-3im@h.u-tokyo.ac.jp

M. Iwabu
Department of Integrated Molecular Science on Metabolic Diseases, 22nd Century Medical and Research Center, Graduate School of Medicine, University of Tokyo, Tokyo, Japan

M. Okada-Iwabu
Department of Molecular Medicinal Sciences on Metabolic Regulation, 22nd Century Medical and Research Center, Graduate School of Medicine, University of Tokyo, Tokyo, Japan

CCL	Chemokine (C-C motif) ligand
CCR	Chemokine (C-C motif) receptor
ERK	Extracellular signal-regulated protein kinase
GTT	Glucose tolerance test
IR-β	Insulin receptor beta
MCP	Monocyte chemoattractant protein
SKM	Skeletal muscles
TG	Triglycerol
WAT	White adipose tissue
WT	Wild-type

Introduction

Obesity is associated with increased infiltration of macrophages into the adipose tissues. These adipose tissue macrophages (ATMs) are currently considered to be a major cause of obesity-associated chronic low-grade inflammation via the secretion of a wide variety of inflammatory molecules [1, 2], including TNF-α, IL-6 [3] and monocyte chemoattractant protein-1 (MCP-1). These inflammatory molecules may have local effects on white adipose tissue (WAT) physiology as well as potential systemic effects on other organs that culminate in insulin resistance.

Among the inflammatory molecules upregulated in the adipose tissues of obese animals and humans, MCP-1 is a member of the cysteine–cysteine (C-C) chemokine family and promotes the migration of inflammatory cells by chemotaxis and integrin activation [4]. Both *Mcp-1* (also known as *Ccl2*) mRNA expression in WAT and plasma MCP-1 levels have been found to correlate positively with the degree of obesity in the individual [5]. In addition, increased production of MCP-1 in WAT precedes the production of other macrophage markers during the development of obesity [6]. Mice overproducing MCP-1 in adipocytes showed macrophage recruitment in WAT and exhibited insulin resistance in the skeletal muscles (SKM) and liver [7]. Regarding the mechanisms, it was reported that MCP-1 stimulates the phosphorylation of extracellular signal-regulated protein kinase (ERK) through the C-C chemokine receptor (CCR) 2 [8] and activation of ERK-1/2 induces insulin resistance via decreased tyrosine phosphorylation of insulin receptor beta (IR-β) [7] as well as increased serine phosphorylation of IRS-1 [9].

Macrophage activation has been operationally defined across two separate polarisation states: M1 and M2. M1, or 'classically activated', macrophages are induced by proinflammatory mediators such as lipopolysaccharide, whereas M2, or 'alternatively activated', macrophages generate high levels of anti-inflammatory cytokines such as IL-10, arginase-1(Arg1), chitinase 3-like 3 (Chi3l3) and TGF-β [10]. It was previously reported that disruption of MCP-1, or its receptor CCR2, in obese mice resulted in decreased macrophage infiltration in WAT and improved metabolic function [11, 12]. Moreover, ATMs from obese *Ccr2*-deficient mice produce M2 markers at levels similar to those seen in lean mice [12]. These data suggest that the MCP-1/CCR2 axis contributes to macrophage polarisation. Therefore, the phenotypic switch in ATM polarisation is thought to lead to amelioration of insulin resistance.

In contrast to obesity, lipoatrophic diabetes is caused by a deficiency of WAT and is characterised by severe hepatic steatosis and insulin resistance. Moitra and colleagues have generated lipoatrophic A-ZIP transgenic (A-ZIP-Tg) mice, which are profoundly insulin resistant and hyperlipidaemic [13–15]. In addition, these mice exhibit severe hepatic steatosis and at the same time a chronic state of inflammation as indicated by high systemic levels of inflammatory cytokines such as IL-1β, IL-6, IL-12 and MCP-1 [16–18]. At the very least, MCP-1 is most abundantly expressed in the liver from A-ZIP-Tg mice [18]. Moreover, treatment of the lipoatrophic A-ZIP-Tg mice with a CCR2 antagonist has been shown to ameliorate the hyperglycaemia, hyperinsulinaemia and hepatomegaly, in conjunction with reducing liver inflammation. However, since CCR2 antagonist can block not only MCP-1, but also MCP-2 (chemokine [C-C motif] ligand [CCL] 8) and MCP-3 (also known as CCL7), it remains unclear whether MCP-1 secreted from liver could contribute to hyperglycaemia, hyperinsulinaemia and hepatomegaly in conjunction with liver inflammation, as well as to M1/M2 polarisation.

In this study, we hypothesised that MCP-1 secreted from the liver might also play an important role in the regulation of macrophage polarisation and insulin resistance-causing kinases such as ERK and p38 mitogen-activated protein kinase (p38MAPK) in liver. To address these issues, we analysed the effects of a targeted disruption of MCP-1 in lipoatrophic A-ZIP-Tg mice. We showed for the first time that a targeted disruption of MCP-1 alone in lipoatrophic diabetic A-ZIP-Tg mice resulted in decreased ERK-1/2 and p38MAPK phosphorylation and increased alternative M2 activation of macrophages, with at the same time an amelioration of insulin resistance and hepatic steatosis.

Methods

Generation of A-ZIP-Tg×Mcp1$^{-/-}$ mice A-ZIP/F-1 (A-ZIP-Tg) mice were generous gifts from C. Vinson of the National Cancer Institute at Frederick, MD, USA. *Mcp1*$^{-/-}$ mice were purchased from the Jackson Laboratory (Bar Harbor, ME, USA) and C57BL/6 mice from CLEA Japan (Fujinomiya, Shizuoka, Japan). A-ZIP/F-1 mice were on an FVB/N (FVB) background. MCP-1 homozygous-knockout mice

were on a C57BL/6 background, which had been backcrossed to C57BL/6 mice for 10 generations.

To generate A-ZIP-Tg *Mcp1*$^{+/-}$ mice, conceptuses that were obtained by in vitro fertilisation of ova from *Mcp1*$^{-/-}$ mice and sperm from A-ZIP-Tg mice were implanted into pseudo-pregnant foster mothers as previously described [19]. To generate A-ZIP-Tg×MCP-1 knockout (*Mcp1*$^{-/-}$) mice and *Mcp1*$^{-/-}$ mice, conceptuses that had been obtained by in vitro fertilisation of ova from MCP-1 homozygous-knockout mice and sperm from A-ZIP-Tg×MCP-1 heterozygous-knockout mice were implanted into pseudo-pregnant foster mothers. To generate wild-type (WT) mice and A-ZIP-Tg mice, conceptuses that had been obtained by in vitro fertilisation of ova from C57BL/6 mice and sperm from A-ZIP-Tg×MCP-1 heterozygous-knockout mice were implanted into pseudo-pregnant foster mothers. All experiments in this study were conducted on female mice.

In this study, we generated WT mice, *Mcp1*$^{-/-}$ mice, A-ZIP-Tg mice and A-ZIP-Tg×*Mcp1*$^{-/-}$ mice which were on an FVB/B6 F2 background. This breeding strategy was used to improve the viability of the offspring as A-ZIP-Tg mice on an FVB background have poor survival [13]. As there was no difference in body weight, plasma glucose levels in the fed state and liver weight between WT mice and *Mcp1*$^{-/-}$ mice (see electronic supplementary material [ESM] Fig. 1), and previous reports had also shown that the body weight, adipose weight, insulin tolerance and glucose tolerance of *Mcp1*$^{-/-}$ mice fed normal chow did not differ from those of WT control mice [11], we analysed and compared the WT mice, A-ZIP-Tg mice and A-ZIP-Tg×*Mcp1*$^{-/-}$ mice. The increase in plasma MCP-1 level of A-ZIP-Tg male mice (ESM Fig. 2a) was similar to that of A-ZIP-Tg female mice (Fig. 1a). MCP-1 deficiency significantly ameliorated hyperglycaemia (ESM Fig. 2b) but not hyperinsulinaemia in A-ZIP-Tg male mice (ESM Fig. 2c). These data suggested that the insulin-sensitive phenotype of A-ZIP-Tg-*Mcp1*$^{-/-}$ mice was prominent in female mice compared with male mice. We thus used female mice in this study.

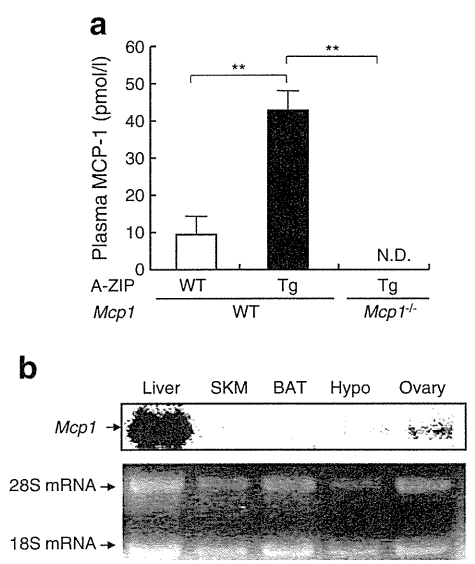

Fig. 1 Plasma MCP-1 concentration and tissue distribution of *Mcp1* mRNA in A-ZIP-Tg mice. (**a**) Plasma concentrations of MCP-1 were measured in WT (white bars), A-ZIP-Tg (black bars) and A-ZIP-Tg×*Mcp1*$^{-/-}$ (grey bars) 15-week-old mice in the fed state. Data are means±SEM. WT mice, n=5; A-ZIP-Tg mice, n=17; A-ZIP-Tg×*Mcp1*$^{-/-}$ mice, n=16. **p<0.01 vs A-ZIP-Tg mice. ND, not detected. (**b**) Northern blot analysis of *Mcp1* mRNA expressed in liver, SKM, BAT, Hypo (hypothalamus) and ovary of 15-week-old A-ZIP-Tg mice

Mice Mice were housed in cages and maintained on a 12-h light/dark cycle. For all experiments, the diet was standard chow (CE-2; CLEA Japan) with the following composition: 25.6% (wt/wt) protein, 3.8% fibre, 6.9% ash, 50.5% carbohydrates, 4% fat and 9.2% water [19–21]. The animal care and use procedures were approved by the Animal Care Committee of the University of Tokyo.

Northern blot analysis Northern blotting was carried out according to the method described previously [20, 21]. Total RNA was extracted from various tissues with TRIzol reagent according to the manufacturer's instructions (Invitrogen, Carlsbad, CA, USA). Total RNA (15 μg) was loaded onto a 1.3% agarose gel and transferred to a nylon membrane (Hybond N+; GE Healthcare Life Sciences, Hino, Tokyo, Japan). MCP-1 coding sequence cDNA was used as the probe template. The cDNA probe template of MCP-1 was prepared by RT-PCR using specific primers. The forward primer was 5′-CCATGCAGGTCCCTGTC-3′ and the reverse primer was 5′-CTAGTTCACTGTCACAC-3′, as previously described [7]. The corresponding bands were quantified by exposure of BAS2000 to the filters and measurement with BAStation software (Fuji Film, Minato-ku, Tokyo, Japan).

Real-time quantitative PCR For real-time quantitative PCR analysis, cDNA synthesised from total RNA was analysed. For quantification of gene expression, a set of predesigned primers and probes for each gene (Assays-on-Demand; Applied Biosystems, Carlsbad, CA, USA) were used. These were mouse MCP-1, Mm00441242_m1; mouse MCP-2: Mm01297183_m1; mouse MCP-3, Mm00443113_m1; mouse CCR2, Mm99999051_gH; mouse Emr1, Mm00802530_m1; mouse CD68, Mm00839636_g1; mouse Chi313, Mm00657889_mH; mouse TGF-β, Mm03024053_m1; mouse Arg1, Mm01190441_g1; mouse PPARa: Mm00440949_m1; mouse Acyl-coA oxidase: Mm00443579_m1; mouse UCP2: Mm00495907_g1; mouse SREBP1c: Mm00550338_m1 and mouse SCD1: Mm00772290_m1.

The primer sets and the probe for mouse cyclophilin were as follows: the forward primer was 5′-GGTCCT GGCATCTTGTCCAT-3′, the reverse primer was 5′-CAGTCTTGGCAGTGCAGATAAAA-3′; and the probe was 5′-CTGGACCAAACACAAACGGTTCCCA-3′. The relative amount of each transcript was normalised to the amount of mouse cyclophilin mRNA.

Blood sample assays and in vivo glucose homeostasis Glucose tolerance tests (GTTs) were conducted as previously described with slight modifications [20, 21]. For the GTTs, mice were deprived of food for 6 h and then orally administered with D-glucose (1.5 g per kg body weight). Plasma glucose and plasma triglycerol (TG) levels in the fed state were determined using a glucose B-test and TG E-type test (Wako Pure Chemical Industries, Yodogawa-ku, Osaka, Japan), respectively. Plasma insulin levels were measured with an insulin immunoassay (Shibayagi, Shibukawa, Gunma, Japan). Plasma MCP-1 levels in the fed state were measured using a mouse immunoassay kit (Pierce Biotechnology, Rockford, IL, USA).

Antibodies Mouse monoclonal anti-phosphotyrosine antibody 4G10 (αPY) was purchased from Merck Millipore (Billerica, MA, USA). Rabbit polyclonal antibody to IR-β was purchased from Santa Cruz Biotechnology (Santa Cruz, CA, USA). Rabbit polyclonal antibodies against ERK-1/2, phospho-ERK-1/2 (Thr202/Tyr204), p38MAPK, phosphor-p38MAPK (Thr180/Tyr182), Akt and phospho-Akt (Ser-473) were purchased from Cell Signaling Technology (Danvers, MA, USA).

Immunoblotting and immunoprecipitation Immunoblotting and immunoprecipitation were conducted as previously described [22]. In brief, in the fed state, the skeletal muscles from the hind limbs or livers were removed. The samples were homogenised in ice-cold 1% Nonidet P-40-buffer (25 mmol/l Tris-HCl [pH 7.4], 10 mmol/l sodium orthovanadate, 10 mmol/l EGTA and 1 mmol/l phenylmethylsulfonyl fluoride) and centrifuged. For immunoblotting, muscle homogenates containing 5 mg of total protein or liver homogenates containing 15 mg of total protein were incubated with the indicated primary antibodies and horseradish peroxidase-conjugated anti-mouse-IgG secondary antibody and were detected with enhanced chemiluminescence (ECL) reagent (GE Healthcare Life Sciences). For immunoprecipitation, muscle homogenates containing 5 mg of total protein or liver homogenates containing 15 mg of total protein were also incubated with the indicated antibodies followed by addition of protein G-Sepharose. The immunoprecipitates were washed with 1% Nonidet P-40-buffer three times. The immunoprecipitates were subjected to immunoblotting with the indicated primary antibodies and horseradish peroxidase-conjugated anti-mouse-IgG secondary antibody and were detected with ECL reagent.

Histological analyses and TG content in liver Livers from WT mice, A-ZIP-Tg mice and A-ZIP-Tg×*Mcp1*$^{-/-}$ mice were fixed overnight in 10% formalin (vol./vol.). Samples were routinely embedded in paraffin. Approximately 5 μm-thick slices obtained from these liver samples were stained with haematoxylin and eosin. The liver homogenates were extracted and their TG content was determined as previously described [19].

Statistical analysis Results are expressed as means±SEM. The Student's *t* test was performed to compare two groups. Data involving more than two groups were assessed by ANOVA. Values of $p<0.05$ were considered statistically significant.

For details of the hyperinsulinaemic–euglycaemic clamp study and antibodies used in immunoprecipitation and immunoblotting, please refer to the ESM Methods.

Results

Plasma MCP-1 concentration and Mcp-1 mRNA expression in fatty liver were increased in lipoatrophic A-ZIP-Tg mice Many previous studies have reported elevated plasma MCP-1 concentration and *Mcp-1* mRNA expression in WAT of obese and diabetic mice [7, 11, 23–25]. As reported [18], plasma MCP-1 concentrations were significantly elevated in A-ZIP-Tg mice compared with WT mice (Fig. 1a). A previous study showed that, in WT mice, *Mcp-1* mRNA was not detected in any tissues [11], whereas in A-ZIP-Tg mice, as previously reported [18], *Mcp-1* mRNA was most abundantly expressed in the liver among all the tissues we examined, including brown adipose tissue (BAT), except for WAT, because lipoatrophic A-ZIP-Tg mice still have BAT but not WAT, as reported in other studies [12–14, 18] (Fig. 1b). It has been reported that MCP-1 is abundantly expressed in Kupffer cells, as well as in hepatocytes in the liver [26, 27]

MCP-1 deficiency decreased body weight gain and liver weight in A-ZIP-Tg mice To clarify the pathophysiological roles of elevated MCP-1 levels in lipoatrophic A-ZIP-Tg mice, we generated A-ZIP-Tg×*Mcp1*$^{-/-}$ mice. MCP-1 deficiency in A-ZIP-Tg mice resulted in decreased body weight compared with A-ZIP-Tg mice (Fig. 2a), although the food intake of A-ZIP-Tg×*Mcp1*$^{-/-}$ mice was not significantly different from that seen in A-ZIP-Tg mice (ESM Table 1). Furthermore, the liver weight of A-ZIP-Tg×*Mcp1*$^{-/-}$ mice was decreased compared with that of A-ZIP-Tg mice (Fig. 2b).

MCP-1 deficiency ameliorated glucose tolerance in lipoatrophic A-ZIP-Tg mice A-ZIP-Tg×*Mcp1*$^{-/-}$ mice showed amelioration of hyperglycaemia, hyperinsulinaemia and hypertriacylglycerolaemia compared with A-ZIP-Tg mice

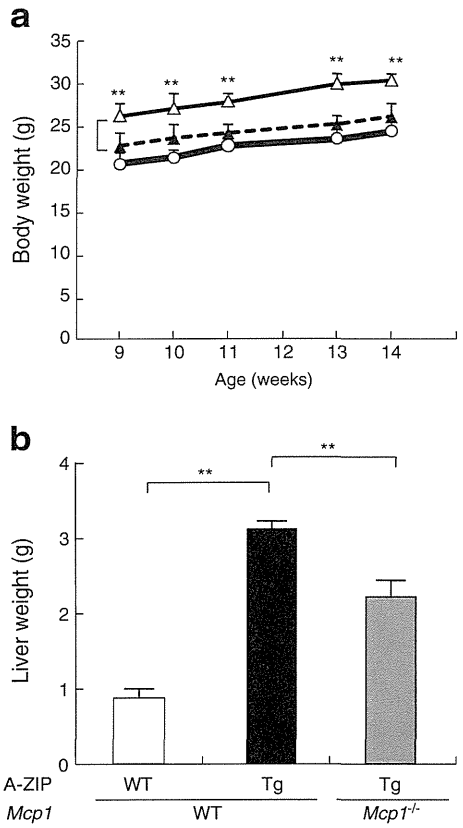

Fig. 2 Body weight and liver weight of WT mice, A-ZIP-Tg mice and A-ZIP-Tg×*Mcp1*$^{-/-}$ mice. (**a**) Body weight of WT mice (white circles), A-ZIP-Tg mice (white triangles) and A-ZIP-Tg×*Mcp1*$^{-/-}$ mice (black triangles) were measured from 9 to 14 weeks of age, as indicated. (**b**) Liver weight of WT (white bars), A-ZIP-Tg (black bars) and A-ZIP-Tg×*Mcp1*$^{-/-}$ (grey bars) in 15-week-old mice. Data are means±SEM. WT mice, n=5; A-ZIP-Tg mice, n=17; A-ZIP-Tg×*Mcp1*$^{-/-}$ mice, n=16. **p<0.01 vs A-ZIP-Tg mice

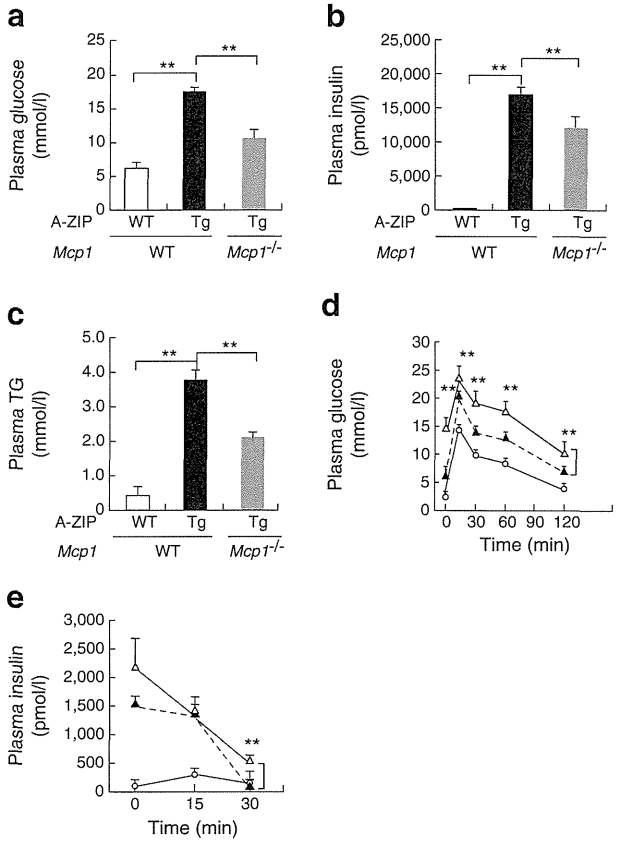

Fig. 3 MCP-1 deficiency in A-ZIP-Tg mice ameliorates glucose intolerance and insulin sensitivity. Plasma values for glucose (**a**), insulin (**b**) and TG (**c**) were measured in 15-week-old WT (white bars), A-ZIP-Tg (black bars) and A-ZIP-Tg×*Mcp1*$^{-/-}$ (grey bars) mice. Plasma glucose (**d**) and plasma insulin (**e**) during GTT (1.5 g glucose per kilogram body weight) in WT (white circles), A-ZIP-Tg (white triangles) and A-ZIP-Tg×*Mcp1*$^{-/-}$ (black triangles) in 15-week-old mice. Data are means±SEM. WT mice, n=5; A-ZIP-Tg mice, n=17; A-ZIP-Tg×*Mcp1*$^{-/-}$ mice, n=16. **p<0.01 vs A-ZIP-Tg mice

(Fig. 3a–c). To further clarify the effects of MCP-1 deficiency in A-ZIP-Tg mice on glucose tolerance and insulin sensitivity, we performed GTTs. Plasma glucose levels and plasma insulin levels during the GTTs were significantly lower in A-ZIP-Tg×*Mcp1*$^{-/-}$ mice than in A-ZIP-Tg mice (Fig. 3d,e), suggesting that MCP-1 deficiency in A-ZIP-Tg mice partially ameliorated glucose intolerance. In WT mice, plasma insulin levels were increased after glucose administration, whereas they were remarkably decreased in A-ZIP-Tg and A-ZIP-Tg- *Mcp1*$^{-/-}$ mice, consistent with previous observations that prolonged hyperinsulinaemia due to severe insulin resistance can result in decreased glucose-stimulated insulin-secretion, in particular decreased early-phase insulin secretion [28]. A hyperinsulinaemic–euglycaemic clamp study revealed that the glucose infusion rate was significantly increased in A-ZIP-Tg- *Mcp1*$^{-/-}$ mice compared with A-ZIP-Tg mice (ESM Fig. 3), indicating that disruption of MCP-1 in A-ZIP-Tg mice could ameliorate insulin resistance.

Livers from A-ZIP-Tg×Mcp1$^{-/-}$ *mice showed increased markers of alternatively activated M2 macrophages* Many studies have demonstrated that macrophage infiltration and levels of proinflammatory cytokines such as MCP-1 and TNF-α are increased in WAT of human obese individuals and several models of rodent obesity [29, 30]. We examined whether the expression of macrophage marker genes would be elevated in other tissues than WAT, such as liver, SKM and BAT, in A-ZIP-Tg mice. The mRNA expressions of *Mcp-1*, *Mcp-3* (*Ccl7*), *Ccr2*, *Emr1* (EGF-like module containing, mucin-like, hormone receptor-like 1) and *Cd68* (CD68 antigen) were increased in the liver (Fig. 4a–e), SKM (ESM Fig. 4) and BAT (ESM Fig. 5) of A-ZIP-Tg mice compared with WT mice. The mRNA expressions of *Mcp-2* were significantly increased in the liver and BAT of A-ZIP-Tg mice compared with those of WT mice. MCP-1 deficiency did not significantly decrease the expressions of *Mcp-2* in the liver, SKM and BAT in A-ZIP-Tg mice (ESM Fig. 6). Unexpectedly, MCP-1

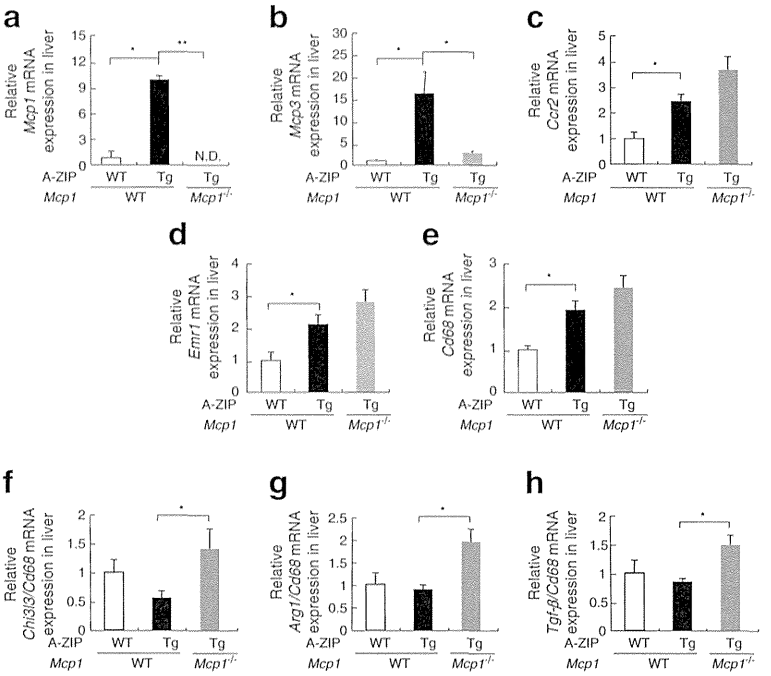

Fig. 4 Effects of MCP-1 deficiency on the expression of macrophage marker genes in liver. *Mcp-1* (**a**), *Mcp-3* (**b**), *Ccr2* (**c**), *Emr1* (**d**) and *Cd68* (**e**) mRNA levels and the mRNA ratio of *Chi3l3/Cd68* (**f**), *Arg1/Cd68* (**g**) and *Tgf-β/Cd68* (**h**) in livers from WT (white bars), A-ZIP-Tg (black bars) and A-ZIP-Tg×*Mcp1*$^{-/-}$ (grey bars) in 15-week-old mice in the fed state were analysed by real-time quantitative PCR. Data are means±SEM. WT mice, n=5; A-ZIP-Tg mice, n=17; A-ZIP-Tg×*Mcp1*$^{-/-}$ mice, n=16. *p<0.05 vs A-ZIP-Tg mice

deficiency did not decrease the expression of macrophage marker genes in other tissues than WAT, such as the liver, SKM and BAT in A-ZIP-Tg mice.

Because a previous report showed that ATMs isolated from obese *Ccr2*-deficient mice expressed alternatively activated M2-macrophage markers [12], we hypothesised that livers from A-ZIP-Tg×*Mcp1*$^{-/-}$ mice might contain M2-polarised macrophages more abundantly. Interestingly, characteristic M2-macrophage marker genes such as *Chi3l3*, *Arg1* and *Tgfb1* were significantly increased in livers from A-ZIP-Tg×*Mcp1*$^{-/-}$ mice (Fig. 4f–h). In contrast to liver, characteristic M2-macrophage marker genes such as *Chi3l3, Arg1* and *Tgfb1* were not significantly changed in SKM and BAT from A-ZIP-Tg×*Mcp1*$^{-/-}$ mice (ESM Fig. 7). Thus, MCP-1 deficiency did not reduce macrophage markers but rather induced macrophages to shift to a M2-polarised state in livers from A-ZIP-Tg mice. These data suggest that MCP-1 deficiency enhances M2 polarisation in livers of A-ZIP-Tg mice.

MCP-1 deficiency decreased liver TG content in A-ZIP-Tg mice It was previously reported that A-ZIP-Tg mice showed dyslipidaemia and severe hepatic steatosis [13]. Liver weights were markedly reduced in A-ZIP-Tg×*Mcp1*$^{-/-}$ mice compared with A-ZIP-Tg mice (Fig. 2b). Representative histological sections of livers showed that MCP-1 deficiency decreased TG accumulation (Fig. 5a). We subsequently determined that the TG content in livers from A-ZIP-Tg×*Mcp1*$^{-/-}$ mice was significantly less than that in livers from A-ZIP-Tg mice (Fig. 5b). To clarify the mechanism by which hepatic steatosis was improved, we studied the expression of genes involved in lipid and energy metabolism and found that expression of *Ppara* mRNA tended to be increased and expression of genes involved in energy dissipation such as *Ucp2* significantly increased in A-ZIP-Tg- *Mcp1*$^{-/-}$ mice compared with A-ZIP-Tg mice, whereas the expression of genes involved in lipogenesis such as *Srebp-1c* (*Srebf1*) and *Scd-1* was not significantly changed (ESM Fig. 8).

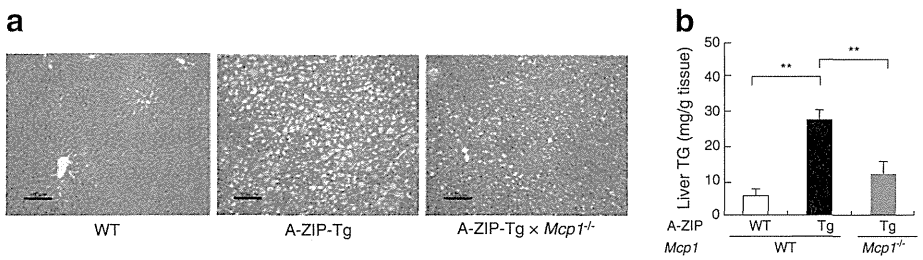

Fig. 5 (**a**) Histological analysis and TG content of liver. Sections of livers were stained with haematoxylin and eosin (Scale bars, 100 μm). (**b**) TG content of livers from WT (white bars), A-ZIP-Tg (black bars) and A-ZIP-Tg×*Mcp1*$^{-/-}$ (grey bars) mice. Data are means±SEM. WT mice, n=5; A-ZIP-Tg mice, n=17; A-ZIP-Tg×*Mcp1*$^{-/-}$ mice, n=16. **p<0.01 vs A-ZIP-Tg mice

MCP-1 deficiency enhanced insulin signalling in livers of A-ZIP-Tg mice Previous studies have reported that MCP-1 induces phosphorylation of ERK through activation of CCR2 in SKM, myocytes, kidney and leukaemia cells [7, 8, 31, 32]. Moreover, Bost et al reported that mice lacking ERK-1 were protected from high-fat diet-induced obesity and insulin resistance [33]. Thus, we hypothesised that inhibition of ERK signalling would improve insulin signalling in A-ZIP-Tg mice, so we studied phosphorylation of ERK-1/2 in livers from A-ZIP-Tg mice and A-ZIP-Tg×*Mcp1*$^{-/-}$ mice. In fact, ERK-1/2 and p38MAPK phosphorylation were significantly increased in livers from A-ZIP-Tg mice compared with WT mice. Conversely, phosphorylation of ERK-1/2 was decreased in livers from A-ZIP-Tg×*Mcp1*$^{-/-}$ mice compared with A-ZIP-Tg mice (Fig. 6a). We next examined the effects of MCP-1 deficiency on insulin signalling in livers from A-ZIP-Tg mice. In livers from A-ZIP-Tg×*Mcp1*$^{-/-}$ mice, tyrosine phosphorylation of IR-β and serine phosphorylation of Akt were significantly increased compared with that seen in A-ZIP-Tg mice (Fig. 7). Moreover, Ser 612 in IRS-1 has been reported to be phosphorylated by ERK [33], which would result in inhibition of insulin signalling. The amount of Ser 612 phosphorylation in IRS-1 was significantly decreased in livers from A-ZIP-Tg×*Mcp1*$^{-/-}$ mice compared with A-ZIP-Tg mice (ESM Fig. 9). Furthermore, in SKM from A-ZIP-Tg×*Mcp1*$^{-/-}$ mice, tyrosine phosphorylation of IR-β was significantly, and serine phosphorylation of Akt tended to be, increased compared with A-ZIP-Tg mice (ESM Fig. 10).

Discussion

MCP-1/CCL2 secreted from WAT in obesity has been reported to contribute to tissue macrophage accumulation and insulin resistance by inducing a chronic inflammatory state. MCP-1 has been shown to be elevated in the fatty liver of lipoatrophic A-ZIP-Tg mice. Treatment of these mice with CCR2 antagonist has been shown to ameliorate their hyperglycaemia, hyperinsulinaemia and hepatomegaly, in conjunction with a reduction in liver inflammation.

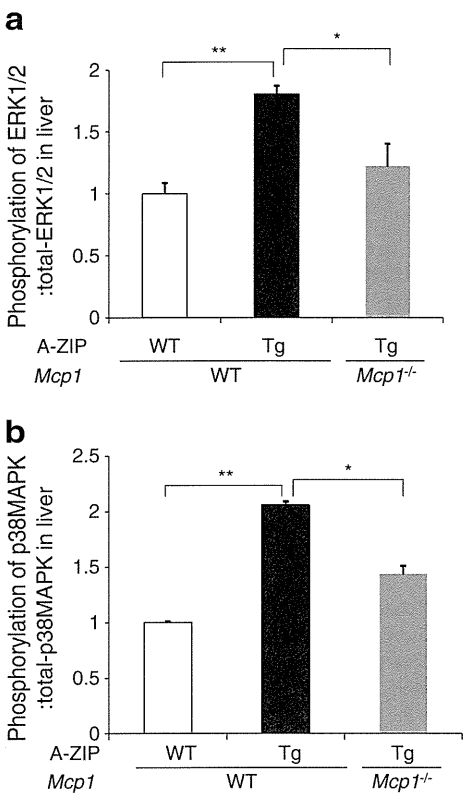

Fig. 6 MCP-1 deficiency in livers from A-ZIP-Tg mice results in the phosphorylation of ERK-1/2 and p38MAPK. Phosphorylation of ERK1/2 (**a**) and p38MAPK (**b**) in livers from WT, A-ZIP-Tg and A-ZIP-Tg×*Mcp1*$^{-/-}$ 15-week-old mice in the fed state were analysed by immunoblotting. The relative amount of each protein was normalised to the total amount of ERK-1/2 or p38MAPK and the ratio is shown. Data are means±SEM (n=3 per group). *p<0.05, **p<0.01 vs WT or A-ZIP-Tg mice

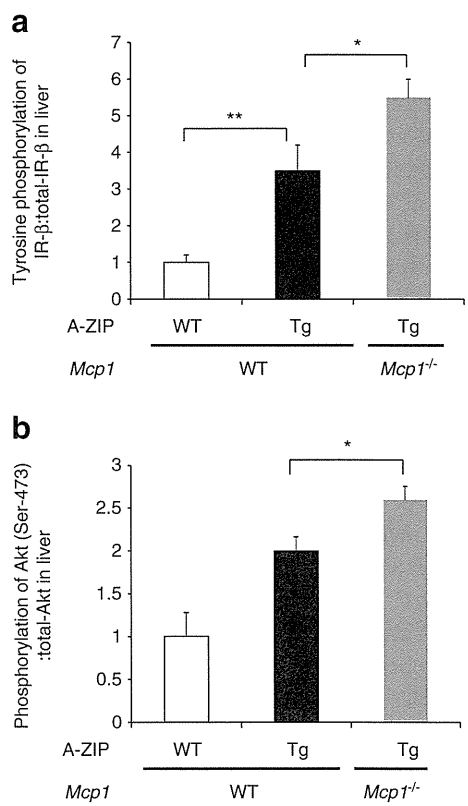

Fig. 7 MCP-1 deficiency in livers from A-ZIP-Tg mice results in increased insulin signalling. Tyrosine phosphorylation of IR-β (**a**) and phosphorylation of Akt (Ser-473) (**b**) in livers from WT, A-ZIP-Tg and A-ZIP-Tg×*Mcp1*$^{-/-}$ 15-week-old mice in the fed state were analysed by immunoblotting. The relative amount of each protein was normalised to the total amount of IR-β or Akt and the ratio is shown. Data are means± SEM (n=3 per group). *p<0.05, **p<0.01 vs WT or A-ZIP-Tg mice

However, since CCR2 antagonist can block not only MCP-1, but also MCP-2 and MCP-3, it remains unclear whether MCP-1 secreted from liver could contribute to hyperglycaemia, hyperinsulinaemia and hepatomegaly in conjunction with liver inflammation, as well as to M1/M2 polarisation.

To address these issues, we analysed the effects of targeted disruption of MCP-1 in A-ZIP-Tg mice. In the current study, we showed for the first time that targeted disruption of MCP-1 alone in lipoatrophic diabetic A-ZIP-Tg mice ameliorated insulin resistance and hepatic steatosis, which was associated with decreased ERK-1/2 and p38MAPK phosphorylation (Fig. 6) and alternative M2 activation of macrophages. Although food intake was not significantly different when adjusted by body weight (ESM Table 1), the A-ZIP-Tg mice with MCP-1 deficiency tended to exhibit increased *Ppara* and exhibited significantly increased *Ucp2* expression in the liver (ESM Fig. 8), raising the possibility that the body weight and liver weight reduction (ESM Table 2) were due to increased energy expenditure, and that it could also contribute to the reduction in liver triacylglycerol content. However, it has been technically extremely difficult to prepare enough A-ZIP-Tg×*Mcp1*$^{-/-}$ mice to unequivocally prove increased energy expenditure in these mice. We would like to carry out this experiment in a future study.

The amounts of tyrosine phosphorylation of IR-β and serine phosphorylation of Akt were increased in livers from A-ZIP-Tg×*Mcp1*$^{-/-}$ mice (Fig. 7). These data suggested that the amelioration of insulin resistance by disruption of MCP-1 in A-ZIP-Tg mice, such as increased tyrosine phosphorylation of IR-β and serine phosphorylation of Akt in liver, seemed to be related to decreased ERK-1/2 and p38MAPK activation [34], at least in part.

Although the disruption of MCP-1 in A-ZIP-Tg mice improved insulin resistance, the gene expression of macrophage markers such as *Emr1* and *Cd68* in the liver were not decreased compared with those seen in A-ZIP-Tg mice (Fig. 4d,e). It was recently reported that the induction of M2 markers in resident macrophages in the liver controls hepatic lipid metabolism [35]. In this study, the M2-specific genes *Chi3l3* and *Arg1* were increased in livers from A-ZIP-Tg×*Mcp1*$^{-/-}$ mice compared with A-ZIP-Tg mice (Fig. 4f,g). These data are consistent with the results that ATMs from obese *Ccr2*-deficient mice express M2 markers at levels similar to those found in lean mice [12]. However, treatment with CCR2 antagonist reduced the macrophage marker gene *Cd68* mRNA and *Tnf-α* mRNA in the livers of A-ZIP-Tg mice [18]. These results might be derived from differences between a chronic and an acute inhibition of CCR2 or between targeted disruption of MCP-1 and simultaneous inhibition of MCP-1/MCP-2/MCP-3 by CCR2 antagonist in the liver of A-ZIP-Tg mice.

Previous studies have shown that CCR2 promoted obesity-induced hepatic steatosis in *db/db* mice [36], that a CCR2 antagonist (propagermanium) also reduced liver TG content in *db/db* mice [37], and that another CCR2 antagonist (RS 504393) ameliorated hepatomegaly but did not decrease hepatic TG content significantly (p=0.144) [18]. These results raised the possibility that inhibition of MCP-1 and/or MCP-2 and/or MCP-3 by CCR2 inhibition could be involved in the suppression of hepatic steatosis. In this study, we showed for the first time that targeted disruption of MCP-1 in A-ZIP-Tg mice by itself exhibited decreased liver TG content in the liver (Fig. 5b), clearly indicating that MCP-1 plays an important role in the onset of hepatic steatosis in the liver in A-ZIP-Tg mice.

In conclusion, we showed for the first time that targeted disruption of MCP-1 by itself ameliorated insulin resistance and hepatic steatosis, and at the same time decreased phosphorylation of ERK-1/2 and p38 MAPK (increased tyrosine phosphorylation of IR-β and serine phosphorylation of Akt) and induced alternative M2 activation of macrophages in the fatty liver from lipoatrophic diabetic A-ZIP-Tg mice. These results suggest that MCP-1 derived from tissues other than WAT, such as fatty liver, could also play an important role in the regulation of whole body insulin sensitivity, hepatic steatosis, macrophage polarisation and phosphorylation of ERK-1/2 and p38 MAPK. The current study also suggests that modulating MCP-1 in the liver would be useful therapy for diabetes and fatty liver.

Acknowledgements We are grateful to K. Miyata for technical assistance.

Funding This work was supported by Grant-in-aid for Scientific Research (S) (20229008) (to T.K.), Grant-in-aid for Scientific Research on Innovative Areas (Research in a proposed research area) 'Molecular Basis and Disorders of Control of Appetite and Fat Accumulation' (to T.Y.), Funding Program for Next Generation World-Leading Researchers (NEXT Program) (to T.Y.), Targeted Proteins Research Program (to T.K.), the Global COE Research Program (to T.K.) and Translational Systems Biology and Medicine Initiative (to T.K.) from the Ministry of Education, Culture, Sports, Science and Technology of Japan.

Duality of interest The authors declare that there is no duality of interest associated with this manuscript.

Contribution statement YN researched, analysed and interpreted data and wrote the manuscript. TY wrote the manuscript, researched, analysed and interpreted data and contributed to the conception and design of this study. MI and MO-I researched, analysed and interpreted data and edited the manuscript. MF and MY researched data and edited the manuscript. KU analysed data and edited the manuscript. TK contributed to the conception and design of this study and edited the manuscript. YN, TY and TK are the guarantors for the content of this article. All authors have approved the final version of the manuscript.

References

1. Wellen KE, Hotamisligil GS (2005) Inflammation, stress, and diabetes. J Clin Invest 115:1111–1119

2. Kershaw EE, Flier JS (2004) Adipose tissue as an endocrine organ. J Clin Endocrinol Metab 89:2548–2556
3. Arranz J, Soriano A, Garcia I et al (2003) Effect of proinflammatory cytokines (IL-6, TNF-alpha, IL-1beta) on hemodynamic performance during orthotopic liver transplantation. Transplant Proc 35:1884–1887
4. Boring L, Gosling J, Cleary M, Charo IF (1998) Decreased lesion formation in CCR2$^{-/-}$ mice reveals a role for chemokines in the initiation of atherosclerosis. Nature 394:894–897
5. Weisberg SP, McCann D, Desai M, Rosenbaum M, Leibel RL, Ferrante AW Jr (2003) Obesity is associated with macrophage accumulation in adipose tissue. J Clin Invest 112:1796–1808
6. Xu H, Barnes GT, Yang Q et al (2003) Chronic inflammation in fat plays a crucial role in the development of obesity-related insulin resistance. J Clin Invest 112:1821–1830
7. Kamei N, Tobe K, Suzuki R et al (2006) Overexpression of monocyte chemoattractant protein-1 in adipose tissues causes macrophage recruitment and insulin resistance. J Biol Chem 281:26602–26614
8. Jimenez-Sainz MC, Fast B, Mayor F Jr, Aragay AM (2003) Signaling pathways for monocyte chemoattractant protein 1-mediated extracellular signal-regulated kinase activation. Mol Pharmacol 64:773–782
9. Gordon S, Taylor PR (2005) Monocyte and macrophage heterogeneity. Nat Rev Immunol 5:953–964
10. Mantovani A, Sica A, Sozzani S, Allavena P, Vecchi A, Locati M (2004) The chemokine system in diverse forms of macrophage activation and polarization. Trends Immunol 25:677–686
11. Kanda H, Tateya S, Tamori Y et al (2006) MCP-1 contributes to macrophage infiltration into adipose tissue, insulin resistance, and hepatic steatosis in obesity. J Clin Invest 116:1494–1505
12. Lumeng CN, Bodzin JL, Saltiel AR (2007) Obesity induces a phenotypic switch in adipose tissue macrophage polarization. J Clin Invest 117:175–184
13. Moitra J, Mason MM, Olive M et al (1998) Life without white fat: a transgenic mouse. Genes Dev 12:3168–3181
14. Gavrilova O, Leon LR, Marcus-Samuels B et al (1999) Torpor in mice is induced by both leptin-dependent and -independent mechanisms. Proc Natl Acad Sci U S A 96:14623–14628
15. Kim JK, Gavrilova O, Chen Y, Reitman ML, Shulman GI (2000) Mechanism of insulin resistance in A-ZIP/F-1 fatless mice. J Biol Chem 275:8456–8460
16. Nunez NP, Oh WJ, Rozenberg J et al (2006) Accelerated tumor formation in a fatless mouse with type 2 diabetes and inflammation. Cancer Res 66:5469–5476
17. Nunez NP, Hursting SD, Yakar S, Fowler D, Vinson C (2009) Obesity provides a permissive milieu in inflammation-associated carcinogenesis: analysis of insulin and IGF pathways. Methods Mol Biol 512:29–37
18. Yang SJ, IglayReger HB, Kadouh HC, Bodary PF (2009) Inhibition of the chemokine (C-C motif) ligand 2/chemokine (C-C motif) receptor 2 pathway attenuates hyperglycaemia and inflammation in a mouse model of hepatic steatosis and lipoatrophy. Diabetologia 52:972–981
19. Yamauchi T, Kamon J, Waki H et al (2003) Globular adiponectin protected ob/ob mice from diabetes and ApoE-deficient mice from atherosclerosis. J Biol Chem 278:2461–2468
20. Yamauchi T, Nio Y, Maki T et al (2007) Targeted disruption of AdipoR1 and AdipoR2 causes abrogation of adiponectin binding and metabolic actions. Nat Med 13:332–339
21. Iwabu M, Yamauchi T, Okada-Iwabu M et al (2010) Adiponectin and AdipoR1 regulate PGC-1alpha and mitochondria by Ca(2+) and AMPK/SIRT1. Nature 464:1313–1319
22. Yamauchi T, Tobe K, Tamemoto H et al (1996) Insulin signalling and insulin actions in the muscles and livers of insulin-resistant, insulin receptor substrate 1-deficient mice. Mol Cell Biol 16:3074–3084
23. Sartipy P, Loskutoff D (2003) Monocyte chemoattractant protein 1 in obesity and insulin resistance. Proc Natl Acad Sci U S A 100:7265–7270
24. Chen A, Mumick S, Zhang C et al (2005) Diet induction of monocyte chemoattractant protein-1 and its impact on obesity. Obes Res 13:1311–1320
25. Li SL, Reddy MA, Cai Q et al (2006) Enhanced proatherogenic responses in macrophages and vascular smooth muscle cells derived from diabetic db/db mice. Diabetes 55:2611–2619
26. Seki E, de Minicis S, Inokuchi S et al (2009) CCR2 promotes hepatic fibrosis in mice. Hepatology 50:185–197
27. Mandrekar P, Ambade A, Lim A, Szabo G, Catalano D (2011) An essential role for monocyte chemoattractant protein-1 in alcoholic liver injury: regulation of proinflammatory cytokines and hepatic steatosis in mice. Hepatology 54:2185–2197
28. Kaneko K, Ueki K, Takahashi N et al (2010) Class IA phosphatidylinositol 3-kinase in pancreatic beta cells controls insulin secretion by multiple mechanisms. Cell Metab 12:619–632
29. Di Gregorio GB, Yao-Borengasser A, Rasouli N et al (2005) Expression of CD68 and macrophage chemoattractant protein-1 genes in human adipose and muscle tissues: association with cytokine expression, insulin resistance, and reduction by pioglitazone. Diabetes 54:2305–2313
30. Chacon MR, Fernandez-Real JM, Richart C et al (2007) Monocyte chemoattractant protein-1 in obesity and type 2 diabetes. Insulin sensitivity study. Obesity (Silver Spring) 15:664–672
31. Dubois PM, Palmer D, Webb ML, Ledbetter JA, Shapiro R (1996) Early signal transduction by the receptor to the chemokine monocyte chemotactic protein-1 in a murine T cell hybrid. J Immunol 156:1356–1361
32. Bost F, Aouadi M, Caron L et al (2005) The extracellular signal-regulated kinase isoform ERK1 is specifically required for in vitro and in vivo adipogenesis. Diabetes 54:402–411
33. Hotamisligil GS (2006) Inflammation and metabolic disorders. Nature 444:860–867
34. Werle M, Schmal U, Hanna K, Kreuzer J (2002) MCP-1 induces activation of MAP-kinases ERK, JNK and p38 MAPK in human endothelial cells. Cardiovasc Res 56:284–292
35. Kang K, Reilly SM, Karabacak V et al (2008) Adipocyte-derived Th2 cytokines and myeloid PPARdelta regulate macrophage polarization and insulin sensitivity. Cell Metab 7:485–495
36. Obstfeld AE, Sugaru E, Thearle M et al (2010) C-C chemokine receptor 2 (CCR2) regulates the hepatic recruitment of myeloid cells that promote obesity-induced hepatic steatosis. Diabetes 59:916–925
37. Tamura Y, Sugimoto M, Murayama T et al (2008) Inhibition of CCR2 ameliorates insulin resistance and hepatic steatosis in db/db mice. Arterioscler Thromb Vasc Biol 28:2195–2201

Original Paper

Intervirology

Intervirology 2013;56:13–21
DOI: 10.1159/000339993

Received: November 1, 2011
Accepted after revision: June 11, 2012
Published online: August 16, 2012

Amino Acid Substitutions in the Hepatitis C Virus Core Region and Lipid Metabolism Are Associated with Hepatocarcinogenesis in Nonresponders to Interferon plus Ribavirin Combination Therapy

Yuya Seko[a] Norio Akuta[a] Fumitaka Suzuki[a] Yusuke Kawamura[a] Hitomi Sezaki[a] Yoshiyuki Suzuki[a] Tetsuya Hosaka[a] Masahiro Kobayashi[a] Mariko Kobayashi[b] Satoshi Saitoh[a] Yasuji Arase[a] Kenji Ikeda[a] Hiromitsu Kumada[a]

[a]Department of Hepatology, and [b]Liver Research Laboratory, Toranomon Hospital, Tokyo, Japan

Key Words
Hepatitis C virus · Genotype · Ribavirin · Interferon · Hepatocellular carcinoma · Core region · High-density lipoprotein cholesterol · IL28B

Abstract
Background: Substitution of amino acid 70 and/or 91 in the core region of hepatitis C virus (HCV) genotype 1b (HCV-1b) is an important predictor of hepatocellular carcinoma (HCC), but its impact on HCC in nonresponders to interferon (IFN) and ribavirin (RIB) combination therapy is not clear. ***Methods:*** A total of 292 patients with HCV-1b-related chronic liver disease who did not achieve a sustained virological response to 24–48 weeks of IFN+RIB combination therapy were included in a follow-up study to investigate the risk factors for HCC. ***Results:*** Sixteen patients developed HCC during the follow-up. The cumulative HCC rates were 5.0, 13.1 and 16.9% at the end of 3, 5 and 7 years, respectively. Multivariate analysis identified substitution of core amino acid 70 (Gln70/His70; hazard ratio 4.64, p = 0.018) and low serum levels of high-density lipoprotein cholesterol (<50 mg/dl; hazard ratio 9.35, p = 0.041) as determinants of HCC. Gender, stage of fibrosis and interleukin-28B showed no such relationship. ***Conclusions:*** Amino acid substitution in the core region of HCV-1b and low serum levels of high-density lipoprotein cholesterol are significant and independent predictors of HCC in nonresponders to IFN+RIB combination therapy. These results emphasize the importance of viral and lipid metabolic factors in the development of HCC after combination therapy.

Introduction

Infection with hepatitis C virus (HCV) is often chronic and can progress to cirrhosis and hepatocellular carcinoma (HCC) [1, 2]. At present, interferon (IFN), in combination with ribavirin (RIB), is the mainstay for treatment of HCV infection. In Japan, more than 70% of HCV infections are caused by HCV genotype 1b (HCV-1b) and are associated with a high viral load, making their treatment difficult [3].

KARGER
Fax +41 61 306 12 34
E-Mail karger@karger.ch
www.karger.com

0300–5526/13/0561–0013$38.00/0

Accessible online at:
www.karger.com/int

Yuya Seko, MD
Department of Hepatology, Toranomon Hospital
2-2-2 Toranomon
Minato-ku, Tokyo 105-0001 (Japan)
Tel. +81 33 588 1111, E-Mail yseko523@toranomon.gr.jp

IFN monotherapy slightly reduces the rates of HCC and normalization of alanine transaminase [4–6]. Furthermore, IFN plus RIB combination therapy also minimizes the risk of HCC, especially among patients who achieve a sustained virological response (SVR) [7]. However, there are currently no suitable factors that could be used to predict HCC in patients who receive the combination therapy but do not achieve SVR.

Several factors have been found to correlate with HCV-related HCC, such as old age, male sex, advanced histopathological stage of liver damage, alcohol intake, HCV genotype and hepatic steatosis [6, 8–12]. Furthermore, mutations in a region spanning amino acids (aa) 2209–2248 within the NS5A protein, the so-called IFN sensitivity-determining region (ISDR) [13], and substitution of aa 70/91 in the core region of HCV-1b [14] as viral-related factors, and genetic variation near the interleukin-28B (IL28B) gene as a host-related factor [15] are also used to predict HCC. The aim of the present study was to identify the viral- and host-related predictive factors for HCC in patients on IFN plus RIB combination therapy (IFN+RIB) who did not achieve SVR. For this purpose, we recruited 292 patients with HCV-related chronic liver disease who did not achieve SVR after 24–48 weeks of IFN+RIB.

Table 1. Profile and laboratory data at the start of IFN+RIB combination therapy of 292 patients infected with HCV-1b who did not achieve SVR

Demographic data	
Number of patients	292
Males/females	144/148
Age, years	56 (20–74)
BMI	22.5 (16.5–40.8)
Laboratory data	
Serum aspartate aminotransferase, IU/l	54 (19–273)
Serum alanine aminotransferase, IU/l	66 (17–504)
Total cholesterol, mg/dl	167 (107–255)
HDL-Chol, mg/dl	48 (24–94)
Low-density lipoprotein cholesterol, mg/dl	95 (35–169)
Triglyceride, mg/dl	93 (28–325)
Platelet count, $\times 10^4/mm^3$	15.0 (6.4–33.1)
Histological findings	
Fibrosis stage F1/F2/F3/F4	77/53/39/1
Amino acid substitutions in HCV-1b	
Core aa 70, arginine/glutamine (histidine)	147/129
Core aa 91, leucine/methionine	139/138
ISDR of NS5A, wild type/non-wild type	217/31
Genetic variation near IL28B gene	
rs8099917 genotype, TT/TG/GG	113/87/4

Data represent numbers of patients or medians (range), as appropriate.

Materials and Methods

Patients

A total of 1,540 HCV-1b-infected adult Japanese patients were consecutively recruited into a study of combination therapy with IFN [IFN or pegylated (PEG)-IFN] plus RIB between March 1999 and October 2010 at Toranomon Hospital, Tokyo, Japan. Among them, 292 were enrolled in this retrospective study. These patients fulfilled the following criteria: (1) positive for anti-HCV (by a third-generation enzyme immunoassay, Chiron Corp., Emeryville, Calif., USA) and HCV RNA by qualitative or quantitative analysis before combination therapy; (2) treated with IFNα-2b or PEG-IFNα-2b plus RIB combination therapy for 24–48 weeks; (3) did not achieve SVR, defined as negative HCV RNA 24 weeks after cessation of antiviral therapy, based on the COBAS TaqMan HCV test (Roche Diagnostics, Tokyo, Japan); (4) free of HCC, both before and during IFN therapy; (5) infected with a single genotype of HCV-1b; (6) negative for hepatitis B surface antigen (by radioimmunoassay, Dainabot, Tokyo, Japan); (7) free of co-infection with the human immunodeficiency virus; (8) lifetime cumulative alcohol intake <500 kg (mild to moderate alcohol intake); (9) free of other types of hepatitis and without hemochromatosis, Wilson disease, primary biliary cirrhosis, alcoholic liver disease and autoimmune liver disease, and (10) had signed a consent form for the study protocol, which had been approved by the human ethics review committee.

Of the total 292 patients, 226 (77%) received PEG-IFNα-2b at a median dose of 1.4 μg/kg (range 1.3–1.9 μg/kg) subcutaneously each week for a median duration of 47 weeks (range 28–48 weeks). The remaining 66 patients (23%) received 6 million units of IFNα-2b intramuscularly for a median duration of 27 weeks (range 24–48 weeks), daily for the initial 2 weeks and then 3 times per week until the last week. The dose of RIB was adjusted according to body weight (600 mg for weight ≤60 kg, 800 mg for weight 60–80 kg and 1,000 mg for weight ≥80 kg).

Table 1 summarizes the profile and laboratory data of the participating patients at the start of combination therapy. The group included 144 males and 148 females aged 20–74 years (median 56 years). The median follow-up period, from the end of antiviral therapy until the last visit, was 1.3 years (range 0.0–8.2 years).

Laboratory Investigations

Blood samples were frozen at –80° within 4 h of collection until used for testing. HCV genotype was determined by PCR using a mixed primer set derived from nucleotide sequences of the NS5 region [16]. Quantitative measurement of HCV RNA was analyzed by the COBAS TaqMan HCV test (Roche Diagnostics). The lower limit of the COBAS TaqMan HCV test is 1.2 log IU/ml, and samples with undetectable levels were defined as negative.

Detection of Amino Acid Substitutions in the Core Region and NS5A Region of HCV-1b

Amino acid substitutions in the core region and NS5A-ISDR of HCV-1b were analyzed by direct sequencing. HCV RNA was

extracted from serum samples at the start of treatment and reverse transcribed with random primer and Moloney murine leukemia virus reverse transcriptase (Takara Syuzo). Nucleic acids were amplified by PCR. For nucleotide sequences of the core region, the first-round PCR was performed with primers CE1 (sense, 5′-GTC TGC GGA ACC GGT GAG TA-3′, nucleotides 134–153) and CE2 (antisense, 5′-GAC GTG GCG TCG TAT TGT CG-3′, nucleotides 1096–1115) and the second-round PCR with primers CC9 (sense, 5′-ACT GCT AGC CGA GTA GTG TT-3′, nucleotides 234–253) and CE6 (antisense, 5′-GGA GCA GTC GTT CGT GAC AT-3′, nucleotides 934–953). For nucleotide sequences of NS5A-ISDR, the first-round PCR was performed with primers ISDR1 (sense, 5′-ATG CCC ATG CCA GGT TCC AG-3′, nucleotides 6662–6681) and ISDR2 (antisense, 5′-AGC TCC GCC AAG GCA GAA GA-3′, nucleotides 7350–7369) and the second-round PCR with primers ISDR3 (sense, 5′-ACC GGA TGT GGC AGT GCT CA-3′, nucleotides 6824–6843) and ISDR4 (antisense, 5′-GTA ATC CGG GCG TGC CCA TA-3′, nucleotides 7189–7208). Nested PCR was used for both the core region and NS5A-ISDR. All samples were initially denatured at 95° for 2 min. The 35 cycles of amplification were set as follows: denaturation for 30 s at 95°, annealing of primers for 30 s at 55° and extension for 1 min at 72° with an additional 7 min for extension. Then, 1 μl of the first PCR product was transferred to the second PCR reaction. Other conditions for the second PCR were the same as the first PCR, except that the second PCR primers were used instead of the first PCR primers. The amplified PCR products were purified by the QIA quick PCR purification kit (Qiagen) after agarose gel electrophoresis and then used for direct sequencing. Dideoxynucleotide termination sequencing was performed with the Big Dye Deoxy Terminator Cycle Sequencing kit (Perkin-Elmer, Tokyo, Japan).

Using HCV-J (accession No. D90208) as a reference [17], the sequence of aa 1–191 in the core protein of HCV-1b was determined and then compared with the consensus sequence constructed on 279 clinical samples to detect substitutions at aa 70 of arginine (Arg70) or glutamine/histidine (Gln70/His70) and at aa 91 of leucine (Leu91) or methionine (Met91) [18]. The sequence of aa 2209–2248 in the NS5A of HCV-1b (ISDR) reported by Enomoto et al. [19] was determined, and the numbers of amino acid substitutions in ISDR were defined as wild type (0) or non-wild type (≥1).

Genetic Variation near the IL28B Gene

Samples for a genome-wide association survey were genotyped using the Illumina HumanHap610-Quad Genotyping BeadChip. Genotyping data were subjected to quality control before data analysis. Genotyping for replication and fine mapping was performed using the Invader assay, TaqMan assay or direct sequencing as described previously [20, 21]. In this study, genetic variations near the IL28B gene (rs8099917), reported as the pretreatment predictors of treatment efficacy and clinical outcome [22–26], were investigated.

Histopathological Examination of the Liver

Liver biopsy specimens were obtained percutaneously or at peritoneoscopy using a modified Vim-Silverman needle with an internal diameter of 2 mm (Tohoku University style, Kakinuma Factory, Tokyo, Japan), fixed in 10% formalin and stained with hematoxylin and eosin, Masson's trichrome, silver impregnation and periodic acid-Schiff after diastase digestion. All specimens for examination contained 6 or more portal areas. Histopathological diagnosis was made by an experienced liver pathologist (H.K.) who was blinded to the clinical data. Chronic hepatitis was diagnosed based on histopathological assessment according to the scoring system of Desmet et al. [27].

Follow-Up and Diagnosis of HCC

Hematological, biochemical and virological tests were performed at least once every month. Imaging studies were conducted every 3 or 4 months in the majority of patients (except those patients who were lost to follow-up); these included computed tomography, magnetic resonance imaging and ultrasonography. If HCC was suspected, additional procedures, such as abdominal angiography and ultrasonography-guided tumor biopsy, if necessary, were used to confirm the diagnosis.

Statistical Analysis

The cumulative rate of HCC was calculated using the Kaplan-Meier technique, and differences in the rates were examined by the log-rank test. Differences in the HCC rate among groups were calculated using the period between the end of combination therapy and appearance of HCC. Stepwise Cox regression analysis was used to determine independent predictive factors associated with HCC. Hazard ratios (HRs) and 95% confidence intervals were also calculated. Potential predictive factors associated with HCC included the following variables: sex, age, type of IFN received, body mass index, platelet count, aspartate aminotransferase, alanine aminotransferase, total cholesterol, high-density lipoprotein cholesterol (HDL-Chol), low-density lipoprotein cholesterol, triglyceride, stage of fibrosis, genetic variation near the IL28B gene and amino acid substitution in the core region and NS5A-ISDR of HCV. Variables that achieved statistical significance ($p < 0.05$) or marginal significance ($p < 0.10$) on univariate analysis were entered into a multivariate Cox proportional hazard model to identify significant independent factors. Statistical comparisons were performed using the SPSS software (SPSS Inc., Chicago, Ill., USA). All p values of less than 0.05 by the two-tailed test were considered significant.

Results

Rate of Hepatocarcinogenesis

During the follow-up, 16 patients (5.4%) developed HCC. The median interval between the end of combination therapy and detection of HCC was 2.0 years (range 0.0–7.6 years). The cumulative rates of HCC were 5.0, 13.2 and 16.9% at the end of 3, 5 and 7 years, respectively.

Predictive Factors Associated with Hepatocarcinogenesis

Data of the entire population sample were analyzed to determine those factors that could predict HCC. Univariate analysis identified 4 parameters that tended to or were significantly correlated with carcinogenesis.

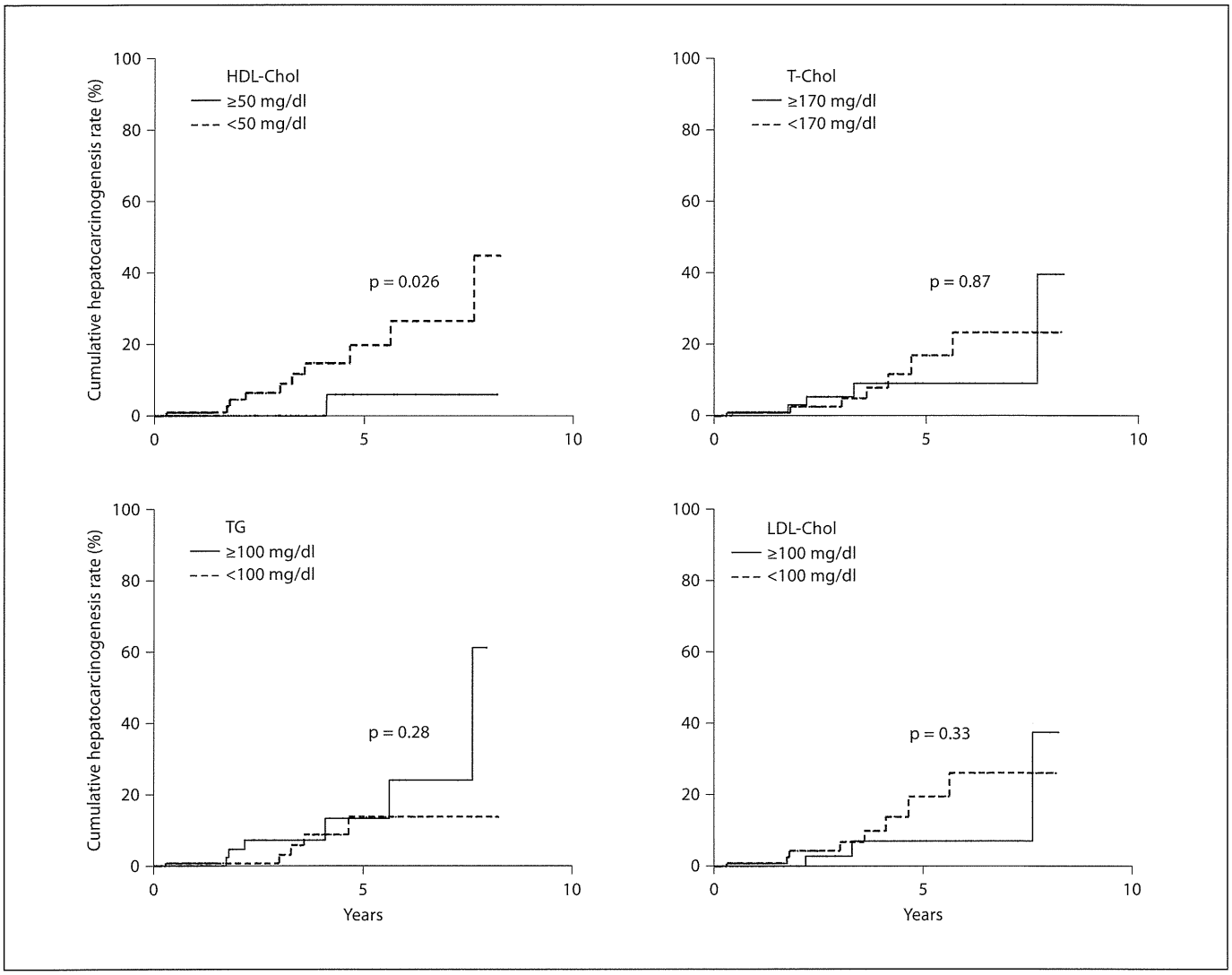

Fig. 1. Cumulative rate of HCC according to serum levels of HDL-Chol, low-density lipoprotein cholesterol (LDL-Chol), total cholesterol (T-Chol) and triglyceride (TG). The rate of HCC was significantly higher for low serum levels of HDL-Chol than high serum levels of HDL-Chol (p = 0.026, log-rank test).

Table 2. Factors associated with hepatocarcinogenesis in patients infected with HCV-1b who did not achieve SVR with IFN+RIB combination therapy, identified by multivariate analysis

Factor	Category	HR	p
Core aa 70	1: Arg70 2: Gln70/His70	1 4.64 (1.30–16.5)	0.018
HDL-Chol	1: ≥50 mg/dl 2: <50 mg/dl	1 9.35 (1.09–83.3)	0.041

Cox proportional hazard model. Values in parentheses represent 95% confidence intervals.

These included age (≥55 years; p = 0.093), body mass index (≥25; p = 0.013), HDL-Chol (<50 mg/dl; p = 0.026) and substitution of aa 70 in the HCV core region (Gln70/His70; p = 0.086). On the other hand, gender, stage of fibrosis and genetic variation near the IL28B gene showed no such correlation. These 4 factors were entered into multivariate analysis, which identified 2 parameters as significant and independent determinants of HCC, namely substitution of aa 70 in the HCV core region (Gln70/His70; HR 4.64, p = 0.018) and serum level of HDL-Chol (<50 mg/dl; HR 9.35, p = 0.041; table 2).

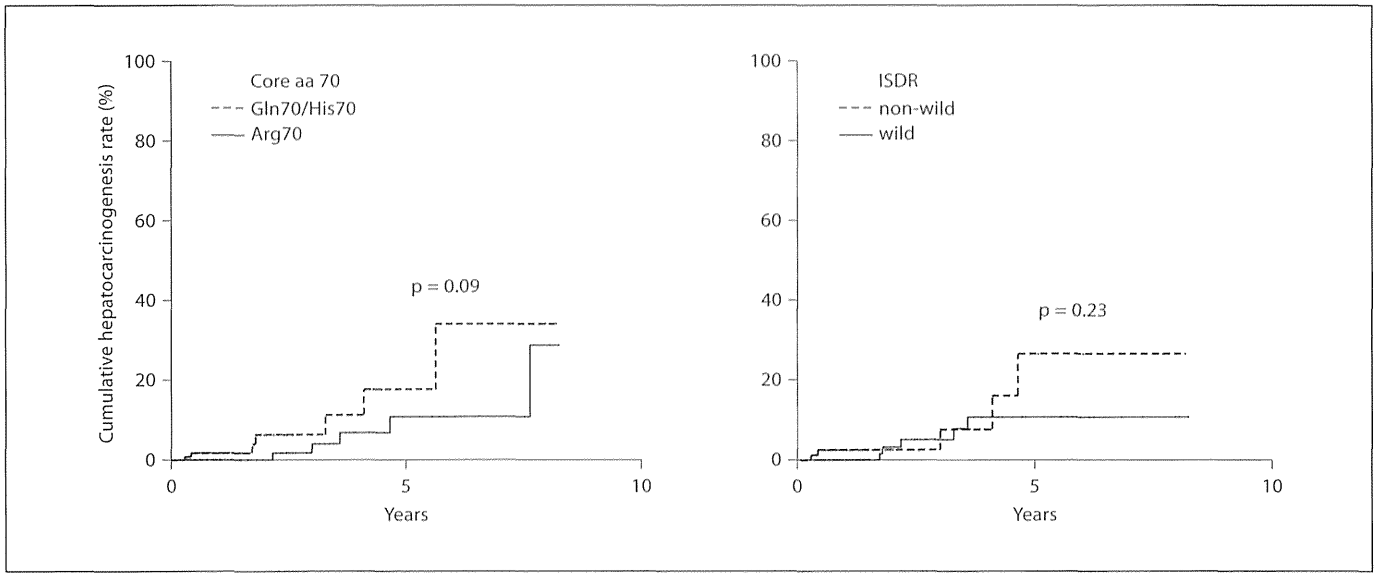

Fig. 2. Cumulative rate of HCC according to amino acid substitutions in the core region of HCV-1b and ISDR of NS5A. The rate of HCC for the Gln70/His70 substitution tended to be higher than that for Arg70 (p = 0.086, log-rank test). There was no significant relationship between ISDR substitution and HCC (p = 0.232, log-rank test).

Rate of HCC according to Substitution of aa 70 in the HCV Core Region and Serum Level of HDL-Chol

The patients were divided into two groups according to the serum level of HDL-Chol using a cutoff value of 50 mg/dl [low HDL-Chol group (<50 mg/dl), n = 127, high HDL-Chol group (≥50 mg/dl), n = 115]. During the follow-up period, 10 patients (8.0%) in the low HDL-Chol group and 1 (1.0%) in the high HDL-Chol group developed HCC. The median interval between the completion of IFN+RIB therapy and detection of HCC was 3.1 years (range 0.0–7.6 years) and 4.1 years for the low and high HDL-Chol groups, respectively. The respective cumulative rates of HCC in the low and high HDL-Chol groups were 9.0 and 0% at the end of 3 years, 19.7 and 5.9% at the end of 5 years, and 26.4 and 5.9% at the end of 7 years. The rates were significantly different between the two groups (p = 0.026, log-rank test; fig. 1).

During the follow-up period, 7 patients (5.7%) who developed HCC had a Gln70/His70 substitution and 5 (3.5%) had an Arg70 substitution. The median interval between the completion of IFN+RIB therapy and detection of HCC in patients with Gln70/His70 and Arg70 was 1.8 years (range 0.0–5.6 years) and 3.6 years (range 0.0–7.6 years), respectively. The respective cumulative rates of HCC in these patients were 6.3 and 4.0% at the end of 3 years, 17.6 and 10.8% at the end of 5 years, and 34.1 and 10.8% at the end of 7 years. The rates tended to be different between the two groups (p = 0.086, log-rank test; fig. 2)

Discussion

Previous studies on Japanese patients infected with HCV-1b reported that IFN+RIB therapy increases the proportion of patients who achieve SVR [3, 28] and that the incidence of HCC among patients who achieve SVR is lower than that among patients who do not [7]. In the present study, we examined the incidence and risk factors of HCC in HCV-1b patients who did not achieve SVR after IFN+RIB therapy. Multivariate analysis identified amino acid substitution in the core region of HCV (Gln70/His70) and serum levels of HDL-Chol (<50 mg/dl) as determinants of HCC in such patients. We also examined the risk factors for HCC in HCV-1b patients treated with IFN+RIB therapy. Multivariate analysis identified age (>55 years), body mass index (>25), ISDR substitutions (wild type), amino acid substitution in the core region of HCV (Gln70/His70) and serum levels of HDL-Chol (<50 mg/dl) as determinants of HCC in such patients (data not shown). This result suggested that the effect of IFN+RIB therapy was independent of amino acid substitution in

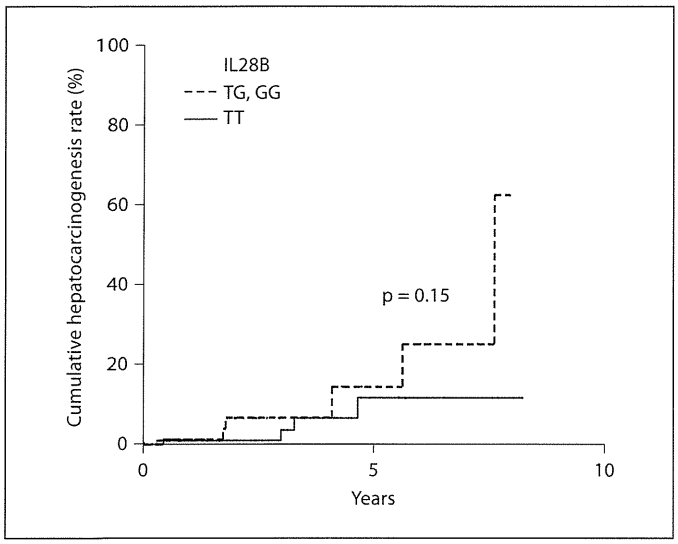

Fig. 3. Cumulative rate of HCC according to genetic variations near the IL28B gene. There was no significant relationship between genetic variations near the IL28B gene and HCC ($p = 0.153$, log-rank test).

the core region and serum levels of HDL-Chol. In this regard, previous reports identified severe fibrosis, male sex, old age, steatosis, HCV genotype [6, 8–12], ISDR substitutions [13], substitution of aa 70 in the HCV core region [14] and IL28B polymorphisms [15] as risk factors for HCC. In the present study, some of the above factors were not identified as significant predictors. The differences between the findings of the present study and the above reports are not clear at present, but they could reflect differences in the population samples, since we focused on Japanese patients with HCV-1b infection who were treated with IFN+RIB therapy and failed to respond to it. Further studies of larger population samples of other ethnicities are necessary.

In this present study, substitution of aa 70 in the HCV core region was associated with the development of HCC after IFN+RIB therapy. Experiments in transgenic mice have provided evidence for the oncogenic role of the HCV core region [29]. Furthermore, patients infected by HCV-1b with amino acid substitutions in the core region are at high risk of HCC [14, 30–32], even after eradication of HCV RNA [33]. In the presence of amino acid substitutions in the core region, IFN-induced phosphorylation of STAT1 and STAT2 is lower, and the expression level of SOCS3, an IFN signal attenuator, was higher than in the wild type. Furthermore, the expression levels of IL-6, which upregulates SOCS3, and those of endoplasmic reticulum stress proteins were significantly higher in cells transfected with core mutant compared with the wild type [34]. These mechanisms may explain the resistance to IFN of HCV-1b with amino acid substitutions in the core region. Other studies also described the important role of a PA28γ-dependent pathway in the development of HCV-associated HCC. Moriishi et al. [35, 36] reported that knockout of the PA28γ gene induces accumulation of HCV core protein in the nuclei of hepatocytes of HCV core gene transgenic mice and disrupts the development of both hepatic steatosis and HCC. Furthermore, HCV core protein is also reported to enhance the binding of liver X receptor α/retinoid X receptor α to liver X receptor response element in the presence of PA28γ [36]. Thus, it seems that PA28γ plays a crucial role in the development of HCV-associated steatosis and HCC. Further studies should be performed to investigate the oncogenic potential of amino acid substitution in the core region of HCV detected at the start of antiviral therapy with regard to HCC after combination therapy.

The relationship between metabolic factors and the risk of HCC is still not clear. Previous studies reported that hepatic steatosis is a significant factor in the development of HCC in HCV-related liver disease independent of age, sex, body mass index, stage of fibrosis and response to antiviral therapy [9, 11]. Other reports indicated that obesity and diabetes mellitus are risk factors for HCC [37–39]. It is also reported that HCV core protein is involved in mitochondrial electron transfer system dysfunction and activation of peroxisome proliferator-activated receptor-α (PPARα). In the presence of mitochondrial dysfunction, PPARα exacerbates steatosis, and persistent activation of PPARα contributes to hepatocarcinogenesis by inducing overproduction of reactive oxygen species and cell growth signal activation [12]. In this present study, multivariate analysis identified amino acid substitution in the core region of HCV and low levels of HDL-Chol as determinants of HCC. These results are not inconsistent with previous studies. Interestingly, in our patients, the impact of amino acid substitution in the core region of HCV and low levels of HDL-Chol was more significant than that of gender, age and stage of fibrosis. One of the reasons for this finding could be the nature of the population study, i.e. Japanese patients treated with IFN+RIB.

Genetic variations near the IL28B gene are pretreatment predictors of a poor virological response to PEG-IFN/RIB combination therapy and triple therapy with telaprevir/PEG-IFN/RIB [22–25, 40]. It has recently been reported that the IL-28B rs12979860 C/T polymorphism

T allele is more prevalent in patients with HCV-related cirrhosis than other etiologies and mild chronic hepatitis C, and also in patients with HCC than in those without HCC [15]. However, the link between IL-28B and HCC remains unclear. In the present study, genetic variations near the IL28B gene did not significantly affect HCC (fig. 3). This discrepant result might be related to differences in the etiology, including hepatitis B virus, alcohol intake and HCV-related liver disease. The population of this study consisted of Japanese patients infected with HCV-1b who were treated with IFN+RIB. Further studies should be conducted to investigate the relationship between genetic variations near the IL28B gene and HCC.

Our study has certain limitations. Firstly, the study did not provide a comprehensive analysis of the viral factors and their role in the development of HCC. Experimental evidence suggests that the pathogenic role of HCV-1b strains in HCC is based on the secondary structure of the amino-terminal portion of the HCV NS3 protein [41]. In the present study, we did not investigate the roles of viral factors except for the HCV core region and NS5A region. Another limitation of the study is the lack of analysis of the clinical impact of lifestyle-related diseases (such as diabetes, insulin resistance, nonalcoholic steatohepatitis) on HCC, except for body mass index and cholesterol levels [38, 39, 42, 43]. Further studies are needed to investigate the clinical impact of viral factors and lifestyle-related diseases on HCC.

We previously indicated that substitution of aa 70 in the HCV-1b core region might predict elevation of serum α-fetoprotein levels in non-HCC patients and that eradication of HCV-1b with Gln70/His70 seemed to induce normalization of α-fetoprotein [44]. To investigate α-fetoprotein during and after PEG-IFN+RIB therapy, according to the substitution pattern of aa 70, is important for evaluating the risk of hepatocarcinogenesis, especially in nonresponders. Further understanding of the complex interaction between α-fetoprotein levels and substitution of aa 70 in the HCV-1b core region should facilitate the development of more effective therapeutic regimens.

In conclusion, the present study identified amino acid substitution in the core region of HCV-1b and low levels of HDL-Chol as significant and independent predictors of HCC in nonresponders to the combination of IFN+RIB. The study emphasizes the importance of viral and lipid metabolic factors in hepatocarcinogenesis after combination therapy.

Acknowledgment

This study was supported in part by a Grant-in-Aid from the Ministry of Health, Labor and Welfare, Japan.

References

1 Niederau C, Lange S, Heintges T, Erhardt A, Buschkamp M, Hürter D, Nawrocki M, Kruska L, Hensel F, Petry W, Häussinger D: Progress of chronic hepatitis C: results of a large, prospective cohort study. Hepatology 1998;28:1687–1695.

2 Kenny-Walsh E: Clinical outcomes after hepatitis C infection from contaminated anti-D immune globulin. Irish Hepatology Research Group. N Engl J Med 1999;340:1228–1233.

3 Tsubota A, Arase Y, Someya T, Suzuki Y, Suzuki F, Saitoh S, Ikeda K, Akuta N, Hosaka T, Kobayashi M, Kumada H: Early viral kinetics and treatment outcome in combination of high-dose interferon induction vs. pegylated interferon plus ribavirin for naive patients infected with hepatitis C virus of genotype 1b and high viral load. J Med Virol 2005;75:27–34.

4 Nishiguchi S, Kuroki T, Nakatani S, Morimoto H, Takeda T, Nakajima S, Shiomi S, Seki S, Kobayashi K, Otani S: Randomized trial of effects of interferon-alpha on incidence of hepatocellular carcinoma in chronic active hepatitis C with cirrhosis. Lancet 1995;346:1051–1055.

5 Yoshida H, Shiratori Y, Moriyama M, Arakawa Y, Ide T, Sata M, Inoue O, Yano M, Tanaka M, Fujiyama S, Nishiguchi S, Kuroki T, Imazeki F, Yokosuka O, Kinoyama S, Yamada G, Omata M: Interferon therapy reduces the risk for hepatocellular carcinoma: national surveillance program of cirrhotic and noncirrhotic patients with chronic hepatitis C in Japan. IHIT Study Group. Inhibition of hepatocarcinogenesis by interferon therapy. Ann Intern Med 1999;131:174–181.

6 Ikeda K, Saitoh S, Arase Y, Chayama K, Suzuki Y, Kobayashi M, Tsubota A, Nakamura I, Murashima N, Kumada H, Kawanishi M: Effect of interferon therapy on hepatocellular carcinogenesis in patients with chronic hepatitis type C: a long-term observation study of 1,643 patients using statistical bias correction with proportional hazard analysis. Hepatology 1999;29:1124–1130.

7 Kurokawa M, Hiramatsu N, Oze T, Mochizuki K, Yakushijin T, Kurashige N, Inoue Y, Igura T, Imanaka K, Yamada A, Oshita M, Hagiwara H, Mita E, Ito T, Inui Y, Hijioka T, Yoshihara H, Inoue A, Imai Y, Kato M, Kiso S, Kanto T, Takehara T, Kasahara A, Hayashi N: Effect of interferon α-2b plus ribavirin therapy on incidence of hepatocellular carcinoma in patients with chronic hepatitis. Hepatol Res 2009;39:432–438.

8 Freeman AJ, Dore GJ, Law MG, Thorpe M, Von Overbeck J, Lloyd AR, Marinos G, Kaldor JM: Estimating progression to cirrhosis in chronic hepatitis C virus infection. Hepatology 2001;34:809–816.

9 Ohata K, Hamasaki K, Toriyama K, Matsumoto K, Saeki A, Yanagi K, Abiru S, Nakagawa Y, Shigeno M, Miyazoe S, Ichikawa T, Ishikawa H, Nakao K, Eguchi K: Hepatic steatosis is a risk factor for hepatocellular carcinoma in patients with chronic hepatitis C virus infection. Cancer 2003;97:3036–3043.

10 Bruno S, Crosignani A, Maisonneuve P, Rossi S, Silini E, Mondelli MU: Hepatitis C virus genotype 1b as a major risk factor associated with hepatocellular carcinoma in patients with cirrhosis: a seventeen-year prospective cohort study. Hepatology 2007;46:1350–1356.

11 Kurosaki M, Hosokawa T, Matsunaga K, Hirayama I, Tanaka T, Sato M, Yasui Y, Tamaki N, Ueda K, Tsuchiya K, Kuzuya T, Nakanishi H, Itakura J, Takahashi Y, Asahina Y, Enomoto N, Izumi N: Hepatic steatosis in chronic hepatitis C is a significant risk factor for developing hepatocellular carcinoma independent of age, sex, obesity, fibrosis stage and response to interferon therapy. Hepatol Res 2010;40:870–877.

12 Koike K, Tsutsumi T, Yotsuyanagi H, Moriya K: Lipid metabolism and liver disease in hepatitis C viral infection. Oncology 2010;78: 24–30.

13 Giménez-Barcons M, Franco S, Suárez Y, Forns X, Ampurdanès S, Puig-Basagoiti F, Sánchez-Fueyo A, Barrera JM, Llovet JM, Bruix J, Sánchez-Tapias JM, Rodés J, Saiz JC: High amino acid variability within the NS5A of hepatitis C virus (HCV) is associated with hepatocellular carcinoma in patients with HCV-1b-related cirrhosis. Hepatology 2001; 34:158–167.

14 Akuta N, Suzuki F, Kawamura Y, Yatsuji H, Sezaki H, Suzuki Y, Hosaka T, Kobayashi M, Kobayashi M, Arase Y, Ikeda K, Kumada H: Amino acid substitutions in the hepatitis C virus core region are the important predictor of hepatocarcinogenesis. Hepatology 2007; 46:1357–1364.

15 Fabris C, Falleti E, Cussigh A, Bitetto D, Fontanini E, Bignulin S, Cmet S, Fornasiere E, Fumolo E, Fangazio S, Cerutti A, Minisini R, Pirisi M, Toniutto P: IL-28B rs12979860 C/T allele distribution in patients with liver cirrhosis: Role in the course of chronic viral hepatitis and the development of HCC. J Hepatol 2011;54:716–722.

16 Chayama K, Tsubota A, Arase Y, Saitoh S, Koida I, Ikeda K, Matsumoto T, Kobayashi M, Iwasaki S, Koyama S, Morinaga T, Kumada H: Genotypic subtyping of hepatitis C virus. J Gastroenterol Hepatol 1993;8:150–156.

17 Kato N, Hijikata M, Ootsuyama Y, Nakagawa M, Ohkoshi S, Sugimura T, Shimotohno K: Molecular cloning of the human hepatitis C virus genome from Japanese patients with non-A, non-B hepatitis. Proc Natl Acad Sci USA 1990;87:9524–9528.

18 Akuta N, Suzuki F, Sezaki H, Suzuki Y, Hosaka T, Someya T, Kobayashi M, Saitoh S, Watahiki S, Sato J, Matsuda M, Kobayashi M, Arase Y, Ikeda K, Kumada H: Association of amino acid substitution pattern in core protein of hepatitis C virus genotype1b high viral load and non-virological response to interferon-ribavirin combination therapy. Intervirology 2005;48:372–380.

19 Enomoto N, Sakuma I, Asahina Y, Kurosaki M, Murakami T, Yamamoto C, Ogura Y, Izumi N, Marumo F, Sato C: Mutations in the nonstructural protein 5A gene and response to interferon in patients with chronic hepatitis C virus 1b infection. N Engl J Med 1996; 334:77–81.

20 Ohnishi Y, Tanaka T, Ozaki K, Yamada R, Suzuki H, Nakamura Y: A high-throughput SNP typing system for genome-wide association studies. J Hum Genet 2001;46:471–477.

21 Suzuki A, Yamada R, Chang X, Tokuhiro S, Sawada T, Suzuki M, Nagasaki M, Nakayama-Hamada M, Kawaida R, Ono M, Ohtsuki M, Furukawa H, Yoshino S, Yukioka M, Tohma S, Matsubara T, Wakitani S, Teshima R, Nishioka Y, Sekine A, Iida A, Takahashi A, Tsunoda T, Nakamura Y, Yamamoto K: Functional haplotypes of PADI4, encoding citrullinating enzyme peptidylarginie deminase 4, are associated with rheumatoid arthritis. Nat Genet 2003;34:395–402.

22 Ge D, Fellay J, Thompson AJ, Simon JS, Shianna KV, Urban TJ, Heinzen EL, Qiu P, Bertelsen AH, Muir AJ, Sulkowski M, McHutchison JG, Goldstein DB: Genetic variation in IL28B predicts hepatitis C treatment-induced viral clearance. Nature 2009;461:399–401.

23 Tanaka Y, Nishida N, Sugiyama M, Kurosaki M, Matsuura K, Sakamoto N, Nakagawa M, Korenaga M, Hino K, Hige S, Ito Y, Mita E, Tanaka E, Mochida S, Murawaki Y, Honda M, Sakai A, Hiasa Y, Nishiguchi S, Koike A, Sakaida I, Imamura M, Ito K, Yano K, Masaki N, Sugauchi F, Izumi N, Tokunaga K, Mizokami M: Genome-wide association of IL28B with response to pegylated interferon-alpha and ribavirin therapy for chronic hepatitis C. Nat Genet 2009;41:1105–1109.

24 Suppiah V, Moldovan M, Ahlenstiel G, Berg T, Weltman M, Abate ML, Bassendine M, Spengler U, Dore GJ, Powell E, Riordan S, Sheridan D, Smedile A, Fragomeli V, Müller T, Bahlo M, Stewart GJ, Booth DR, George J: IL28B is associated with response to chronic hepatitis C interferon-alpha and ribavirin therapy. Nat Genet 2009;41:1100–1104.

25 Rauch A, Kutalik Z, Descombes P, Cai T, Di Iulio J, Mueller T, Bochud M, Battegay M, Bernasconi E, Borovicka J, Colombo S, Cerny A, Dufour JF, Furrer H, Günthard HF, Heim M, Hirschel B, Malinverni R, Moradpour D, Müllhaupt B, Witteck A, Beckmann JS, Berg T, Bergmann S, Negro F, Telenti A, Bochud PY: Genetic variation in IL28B is associated with chronic hepatitis C and treatment failure: a genome-wide association study. Gastroenterology 2010;138:1338–1345.

26 Thomas DL, Thio CL, Martin MP, Qi Y, Ge D, O'Huigin C, Kidd J, Kidd K, Khakoo SI, Alexander G, Goedert JJ, Kirk GD, Donfield SM, Rosen HR, Tobler LH, Busch MP, McHutchison JG, Goldstein DB, Carrington M: Genetic variation in IL28B and spontaneous clearance of hepatitis C virus. Nature 2009;8;461:798–801.

27 Desmet VJ, Gerber M, Hoofnagle JH, Manna M, Scheuer PJ: Classification of chronic hepatitis: Diagnosis, grading and staging. Hepatology 1994;19:1513–1520.

28 Akuta N, Suzuki F, Kawamura Y, Yatsuji H, Sezaki H, Suzuki Y, Hosaka T, Kobayashi M, Kobayashi M, Arase Y, Ikeda K, Kumada H: Predictive factors of early and sustained responses to peginterferon plus ribavirin combination therapy in Japanese patients infected with hepatitis C virus genotype 1b: amino acid substitutions in the core region and low-density lipoprotein cholesterol levels. J Hepatol 2007;46:403–410.

29 Moriya K, Fujie H, Shintani Y, Yotsuyanagi H, Tsutsumi T, Ishibashi K, Matsuura Y, Kimura S, Miyamura T, Koike K: The core protein of hepatitis C virus induces hepatocellular carcinoma in transgenic mice. Nat Med 1998;4:1065–1067.

30 Fishman SL, Factor SH, Balestrieri C, Fan X, Dibisceglie AM, Desai SM, Benson G, Branch AD: Mutations in the hepatitis C virus core gene are associated with advanced liver disease and hepatocellular carcinoma. Clin Cancer Res 2009;15:3205–3213.

31 Hu Z, Muroyama R, Kowatari N, Chang J, Omata M, Kato N: Characteristic mutations in hepatitis C virus core gene related to the occurrence of hepatocellular carcinoma. Cancer Sci 2009;100:2465–2468.

32 Nakamoto S, Imazeki F, Fukai K, Fujiwara K, Arai M, Kanda T, Yonemitsu Y, Yokosuka O: Association between mutations in the core region of hepatitis C virus genotype 1 and hepatocellular carcinoma development. J Hepatol 2010;52:72–78.

33 Akuta N, Suzuki F, Hirakawa M, Kawamura Y, Sezaki H, Suzuki Y, Hosaka T, Kobayashi M, Kobayashi M, Saitoh S, Arase Y, Ikeda K, Kumada H: Amino acid substitutions in hepatitis C virus core region predict hepatocarcinogenesis following eradication of HCV RNA by antiviral therapy. J Med Virol 2011; 83:1016–1022.

34 Funaoka Y, Sakamoto N, Suda G, Itsui Y, Nakagawa M, Kakinuma S, Watanabe T, Mishima K, Ueyama M, Onozuka I, Nitta S, Kitazume A, Kiyohashi K, Murakawa M, Azuma S, Tsuchiya K, Watanabe M: Analysis of interferon signaling by infectious hepatitis C virus clones with substitutions of core amino acids 70 and 91. J Virol 2011;85:5986–5994.

35 Moriishi K, Okabayashi T, Nakai K, Moriya K, Koike K, Murata S, Chiba T, Tanaka K, Suzuki R, Suzuki T, Miyamura T, Matsuura Y: Proteasome activator PA28gamma-dependent nuclear retention and degradation of hepatitis C virus core protein. J Virol 2003; 77:10237–10249.

36 Moriishi K, Mochizuki R, Moriya K, Miyamoto H, Mori Y, Abe T, Murata S, Tanaka K, Miyamura T, Suzuki T, Koike K, Matsuura Y: Critical role of PA28gamma in hepatitis C virus-associated steatogenesis and hepatocarcinogenesis. Proc Natl Acad Sci USA 2007;104:1661–1666.

▶37 Polesel J, Zucchetto A, Montella M, Dal Maso L, Crispo A, La Vecchia C, Serraino D, Franceschi S, Talamini R: The impact of obesity and diabetes mellitus on the risk of hepatocellular carcinoma. Ann Oncol 2009;20:353–357.
▶38 Kawamura Y, Arase Y, Ikeda K, Hirakawa M, Hosaka T, Kobayashi M, Saitoh S, Yatsuji H, Sezaki H, Akuta N, Suzuki F, Suzuki Y, Kumada H: Diabetes enhances hepatocarcinogenesis in noncirrhotic, interferon-treated hepatitis C patients. Am J Med 2010;123:951–956.
▶39 Sumida Y, Kanemasa K, Hara T, Inada Y, Sakai K, Imai S, Yoshida N, Yasui K, Itoh Y, Okanoue T, Yoshikawa T: Impact of amino acid substitutions in hepatitis C virus genotype 1b core region on liver steatosis and glucose tolerance in non-cirrhotic patients without overt diabetes. J Gastroenterol Hepatol 2011;26:836–842.
▶40 Akuta N, Suzuki F, Hirakawa M, Kawamura Y, Yatsuji H, Sezaki H, Suzuki Y, Hosaka T, Kobayashi M, Kobayashi M, Saitoh S, Arase Y, Ikeda K, Chayama K, Nakamura Y, Kumada H: Amino acid substitution in HCV core region and genetic variation near the interleukin 28B gene predict viral response to telaprevir with peginterferon and ribavirin. Hepatology 2010;52:421–429.
▶41 Ogata S, Florese RH, Nagano-Fujii M, Hidajat R, Deng L, Ku Y, Yoon S, Saito T, Kawata S, Hotta H: Identification of hepatitis C virus (HCV) subtype 1b strains that are highly, or only weakly, associated with hepatocellular carcinoma on the basis of the secondary structure of an amino-terminal portion of the HCV NS3 protein. J Clin Microbiol 2003;41:2835–2841.
▶42 Mason AL, Lau JY, Hoang N, Qian K, Alexander GJ, Xu L, Guo L, Jacob S, Regenstein FG, Zimmerman R, Everhart JE, Wasserfall C, Maclaren NK, Perrillo RP: Association of diabetes mellitus and chronic hepatitis C virus infection. Hepatology 1999;29:328–333.
▶43 El-Serag HB, Tran T, Everhart JE: Diabetes increases the risk of chronic liver disease and hepatocellular carcinoma. Gastroenterology 2004;126:460–468.
▶44 Akuta N, Suzuki F, Kawamura Y, Yatsuji H, Sezaki H, Suzuki Y, Hosaka T, Kobayashi M, Kobayashi M, Arase Y, Ikeda K, Kumada H: Substitution of amino acid 70 in the hepatitis C virus core region of genotype 1b is an important predictor of elevated alpha-fetoprotein in patients without hepatocellular carcinoma. J Med Virol 2008;80:1354–1362.

HEPATOLOGY
Official Journal of the American Association for the Study of Liver Diseases

Effect of Type 2 Diabetes on Risk for Malignancies Includes Hepatocellular Carcinoma in Chronic Hepatitis C

Yasuji Arase,[1-3] Mariko Kobayashi,[1] Fumitaka Suzuki,[1] Yoshiyuki Suzuki,[1] Yusuke Kawamura,[1] Norio Akuta,[1] Masahiro Kobayashi,[1] Hitomi Sezaki,[1] Satoshi Saito,[1] Tetsuya Hosaka,[1] Kenji Ikeda,[1] Hiromitsu Kumada,[1] and Tetsuro Kobayashi[3]

The aim of this retrospective cohort study was to assess the cumulative development incidence and predictive factors for malignancies after the termination of interferon (IFN) therapy in Japanese patients for hepatitis C virus (HCV). A total of 4,302 HCV-positive patients treated with IFN were enrolled. The mean observation period was 8.1 years. The primary outcome was the first onset of malignancies. Evaluation was performed using the Kaplan-Meier method and Cox proportional hazard analysis. A total of 606 patients developed malignancies: 393 developed hepatocellular carcinoma (HCC) and 213 developed malignancies other than HCC. The cumulative development rate of HCC was 4.3% at 5 years, 10.5% at 10 years, and 19.7% at 15 years. HCC occurred significantly ($P < 0.05$) when the following characteristics were present: advanced histological staging, sustained virological response not achieved, male sex, advanced age of ≥50 years, total alcohol intake of ≥200 kg, and presence of type 2 diabetes (T2DM). T2DM caused a 1.73-fold enhancement in HCC development. In patients with T2DM, HCC decreased when patients had a mean hemoglobin A1c (HbA1c) level of <7.0% during follow-up (hazard ratio, 0.56; 95% confidence interval, 0.33-0.89; $P = 0.015$). The cumulative development rate of malignancy other than HCC was 2.4% at 5 years, 5.1% at 10 years, and 9.8% at 15 years. Malignancies other than HCC occurred significantly when patients were of advanced age of ≤50 years, smoking index (package per day × year) was ≥ 20, and T2DM was present. T2DM caused a 1.70-fold enhancement in the development of malignancies other than HCC. *Conclusion:* T2DM causes an approximately 1.7-fold enhancement in the development of HCC and malignancies other than HCC in HCV-positive patients treated with IFN. In T2DM patients, maintaining a mean HbA1c level of <7.0% reduces the development of HCC. (HEPATOLOGY 2013;57:964-973)

Hepatitis C virus (HCV) is one of the more common causes of chronic liver disease worldwide. Chronic hepatitis C is an insidiously progressive form of liver disease that relentlessly but silently progresses to cirrhosis in 20%-50% of cases over a period of 10-30 years.[1,2] In addition, HCV is a major risk factor for hepatocellular carcinoma (HCC).[3-7]

On the other hand, the prevalence of patients with type 2 diabetes mellitus (T2DM) is increasing in many nations, including Japan.[8] Thus, the management of T2DM patients who are chronically infected with HCV is one of the most important issues confronted by physicians. Few studies have reported relationships between T2DM and total malignancies, including HCC in HCV patients. In addition, it is not clear whether the stringent control of T2DM is necessary for protecting the development of malignancies in HCV patients. This issue needs to be confirmed via long-term follow-up of a large cohort of patients at high risk of developing malignancy.

Abbreviations: CH, chronic hepatitis; CI, confidence interval; HbA1c, hemoglobin A1c; HCC, hepatocellular carcinoma; HCV, hepatitis C virus; HR, hazard ratio; IFN, interferon; LC, liver cirrhosis; SVR, sustained virological response; T2DM, type 2 diabetes mellitus; TAI, total alcohol intake.

From the [1]Department of Hepatology and Okinaka Memorial Institute for Medical Research, Toranomon Hospital, Tokyo, Japan; the [2]Department of Health Management Center, Toranomon Hospital, Tokyo, Japan; and the [3]Department of Third Internal Medicine, University of Yamanashi, Yamanashi, Japan.

Received May 4, 2012; accepted September 7, 2012.

This work was supported in part by the Japanese Ministry of Health, Labour and Welfare.